

0294
MASTER COPY

DEC 13 1994

ORNL/NRC/LTR-94/38

**DEVELOPMENT OF THE BWR DRY CORE
INITIAL AND BOUNDARY CONDITIONS
FOR THE SNL XR2 EXPERIMENTS**

F. P. Griffin L. J. Ott

**Boiling Water Reactor Experimental Analysis and Model
Development for Severe Accidents Program**

**Oak Ridge National Laboratory
Oak Ridge, Tennessee**

Letter Report

October 31, 1994

Research sponsored by the U.S. Nuclear Regulatory Commission, Office of Nuclear Regulatory Research under Interagency Agreement DOE 1886-8620-2W with the U.S. Department of Energy under contract DE-AC05-84OR21400 with the Martin Marietta Energy Systems, Inc.

Notice

This report was prepared as an account of work sponsored by an agency of the United States Government. Neither the United States Government nor any agency thereof, or any of their employees, makes any warranty, expressed or implied, or assumes any legal liability or responsibility for any third party's use, or the results of such use, of any information, apparatus, product or process disclosed in this report, or represents that its use by such third part would not infringe privately owned rights.

**DEVELOPMENT OF THE BWR DRY CORE
INITIAL AND BOUNDARY CONDITIONS
FOR THE SNL XR2 EXPERIMENTS**

F. P. Griffin L. J. Ott

**Boiling Water Reactor Experimental Analysis and Model
Development for Severe Accidents Program**

**Oak Ridge National Laboratory
Oak Ridge, Tennessee**

Letter Report

October 31, 1994

Research sponsored by the U.S. Nuclear Regulatory Commission, Office of Nuclear Regulatory Research under Interagency Agreement DOE 1886-8620-2W with the U.S. Department of Energy under contract DE-AC05-84OR21400 with the Martin Marietta Energy Systems, Inc.

Notice

This report was prepared as an account of work sponsored by an agency of the United States Government. Neither the United States Government nor any agency thereof, or any of their employees, makes any warranty, expressed or implied, or assumes any legal liability or responsibility for any third party's use, or the results of such use, of any information, apparatus, product or process disclosed in this report, or represents that its use by such third part would not infringe privately owned rights.

CONTENTS

	<u>Page</u>
1. INTRODUCTION	1-1
2. XR EXPERIMENTS	2-1
2.1 BWR DRY CORE ACCIDENT SCENARIO	2-1
2.2 XR TEST DESCRIPTION	2-2
2.3 PEER REVIEW COMMENTS ON THE EX-REACTOR EXPERIMENTS .	2-4
2.4 ORNL SUPPORT OF THE XR2 TEST SERIES	2-5
3. SCDAP/RELAP5 MODEL FOR BROWNS FERRY	3-1
3.1 DESCRIPTION OF BASIC MODEL	3-1
3.1.1 Hydrodynamic Nodalization	3-1
3.1.2 Structure Models	3-2
3.1.3 Decay Power Distribution	3-2
3.1.4 STSB Accident Sequence	3-3
3.2 MODEL TO REPRESENT FUEL BUNDLE TEMPERATURE DISTRIBUTION	3-4
3.3 MODEL VERIFICATION	3-5
4. INITIAL AND BOUNDARY CONDITIONS FOR THE XR2 TESTS	4-1
4.1 BROWNS FERRY STSB TRANSIENT	4-1
4.2 INITIAL THERMAL CONDITIONS	4-2
4.3 BOUNDARY CONDITIONS	4-2
5. SUMMARY	5-1
6. REFERENCES	6-1

DEVELOPMENT OF THE BWR DRY CORE INITIAL AND BOUNDARY CONDITIONS FOR THE SNL XR2 EXPERIMENTS

F. P. Griffin L. J. Ott

**Boiling Water Reactor Experimental Analysis and Model Development for Severe Accidents Program
Oak Ridge National Laboratory
Oak Ridge, Tennessee**

1. INTRODUCTION

The objectives of the Boiling Water Reactor Experimental Analysis and Model Development for Severe Accidents (BEAMD) Program at the Oak Ridge National Laboratory (ORNL) are: (1) the development of a sound quantitative understanding of boiling water reactor (BWR) core melt progression; this includes control blade and channel box effects, metallic melt relocation and possible blockage formation under severe accident conditions, and (2) provision of BWR melt progression modeling capabilities in SCDAP/RELAP5 (consistent with the BWR experimental data base).

This requires the assessment of current modeling of BWR core melt progression against the expanding BWR data base. Emphasis is placed upon data from the BWR tests in the German CORA test facility and from the ex-reactor experiments [Sandia National Laboratories (SNL)] on metallic melt relocation and blockage formation in BWRs, as well as upon in-reactor data from the Annular Core Research Reactor (ACRR) DF-4 BWR test (conducted in 1986 at SNL).

The BEAMD Program is a derivative of the BWR Severe Accident Technology Programs at ORNL. The ORNL BWR programs have studied postulated severe accidents in BWRs and have developed a set of models¹ specific to boiling water reactor response under severe accident conditions. These models, in an experiment-specific format, have been successfully applied to both pretest and posttest analyses of the DF-4 experiment,^{2,3} and the BWR severe fuel damage (SFD) experiments⁴⁻⁷ performed in the CORA facility at the Kernforschungszentrum Karlsruhe (KfK) in Germany, resulting in excellent agreement between model prediction and experiment.

The ORNL BWR models have provided far more precise predictions of the conditions in the BWR experiments than were previously available. This has provided a basis for more accurate interpretation of the phenomena for which the experiments are performed. The experiment-specific models, as used in the ORNL DF-4 and CORA BWR experimental analyses, also provide a basis for the efficient development of new models for phenomena such as materials interaction; and these validated phenomenological models (from the results of the experiments) then may be incorporated in the systems-level codes (MELCOR⁸ and SCDAP/RELAP5⁹).

Improved structural models for the BWR canister/control blade,¹⁰⁻¹¹ simplified versions of the CORA BWR experiment-specific models, have been incorporated into the SCDAP/RELAP5 code.

In accordance with Task 5 of the Form 189 for JCN W6202, dated September 15, 1994, the ORNL BEAMD Program is to continue to interact with SNL and provide analytical support to SNL for the XR2 series of tests (under JCN L1468 at SNL) on metallic melt relocation and blockage formation under BWR accident conditions. Initial and boundary conditions for the XR2-1 experiment are to be obtained by means of SCDAP/RELAP5 calculations based upon the Browns Ferry station blackout accident sequence.

It is the purpose of this letter report to present the results of the best-estimate SCDAP/RELAP5 calculations and to provide recommended initial and boundary conditions for the SNL XR2 ex-reactor experiments. Chapter 2 will focus on the description of the BWR dry-core accident scenario and the SNL ex-reactor experiments. Chapter 3 briefly describes the ORNL SCDAP/RELAP5 Browns Ferry model. Chapter 4 will discuss the results of the ORNL analysis.

Chapter 5 provides a summary of the main points of this report. References cited are listed in Chapter 6.

This report is in partial fulfillment of Task 5 of the NRC Form 189 for JCN W6202 dated September 15, 1994.

2. XR EXPERIMENTS

2.1 BWR DRY CORE ACCIDENT SCENARIO¹²

Review of the results of probabilistic risk assessment (PRA) demonstrates conclusively that the BWR is vulnerable only to loss of reactor vessel injection and that the postulated accident sequence scenarios leading to core damage always involve means for failure of function of the vessel injection systems. As defined, the various severe accident sequences involve different pathways to and timing of loss of vessel injection capability but, in every case, the core must become uncovered before core damage can occur.

The Station Blackout accident sequence has consistently been identified as the leading contributor to the calculated core damage frequency in recent PRAs for plants of the BWR design. BWRs are well protected against core damage because they have redundant reactor vessel injection systems to keep the core covered with water. The reason that Station Blackout is the leading contributor to BWR core damage frequency is simply that the majority of the reactor vessel injection systems are dependent upon the availability of alternate current (AC) power and BWRs are vulnerable to loss of injection.

Station Blackout is the accident sequence initiated by loss of off-site AC power and the associated scram and closure of the main steam isolation valves combined with failure of the station diesels (or gas turbines) to start and load. Therefore, all electric motor-driven reactor injection systems become unavailable at the inception of the accident sequence.

Most of the 37 operating BWR facilities in the United States are protected against loss of the motor-driven reactor vessel injection systems by having steam turbine-driven injection systems. Since these systems rely upon direct current (DC) power for valve operation and turbine governor control, they will eventually be lost if AC power is not restored before the unit batteries become exhausted. The sequence with successful operation of the turbine-driven injection systems is classified as Long-Term Station Blackout because a significant period of time (typically six to eight hours) would elapse before battery exhaustion caused loss of reactor vessel injection capability and means for operator control of pressure. The characteristics of this sequence (Figure 2.1) are (1) loss of injection, (2) loss of ability to manually manipulate the safety relief valves (SRVs) after battery failure, (3) vessel pressure dependent on SRV automatic actuations, (4) boiloff, and (5) core steaming dominated by SRV actuations. This sequence is termed a "wet" core degradation scenario; that is, during the core degradation process there is water within the core with continuous steaming that can feed metal/steam oxidation reactions.

The second form of the severe accident sequence associated with loss of all AC power is termed Short-Term Station Blackout (STSB) because for this sequence, the steam turbine-driven injection systems fail to start upon demand. However, DC power is available for SRV actuation so that the operators can take meaningful action in following the Emergency Procedure Guidelines (EPGs).

The basic functional goal of the EPGs is to establish the prudent actions to be taken by the operators in response to the symptoms observed by them at any point in time. Once entry into the EPGs has occurred, the operators are expected to take the specified actions regardless of equipment design bases limitations or licensing commitments. The guidelines use multiple mitigation strategies wherever possible so that recovery from an abnormal situation does not require successful operation of any one system or component.

In the STSB scenario, if AC power is not restored, partial uncovering of the core will occur and, per the EPGs, the operators will initiate the "steam cooling" maneuver. The purpose of this maneuver is to delay fuel heatup by cooling the uncovered upper regions of the core by a rapid flow of steam. Since the source of the steam is the remaining inventory of water in the reactor vessel, however, the steam cooling maneuver provides only a temporary delay (10 to 20 minutes) in core heatup and concludes with a vessel water level below the core plate. (The core plate is located ~23 cm below the active fissile region of the core.) The characteristics of this sequence (Figure 2.2) are (1) no injection, (2) vessel depressurized, (3) boiloff with flashing during depressurization, and (4) steam-starved core degradation. This sequence is termed a "dry" core degradation scenario because core degradation occurs under minimal steaming conditions with essentially a stagnant, steam-starved core atmosphere.

All BWR degraded core experiments performed prior to CORA-33⁶ (October 1992) were conducted under "wet" core degradation conditions for which water remains within the core and continuous steaming feeds metal/steam oxidation reactions on the in-core metallic surfaces. Thus, one dominant set of accident scenarios, the "dry" core sequence, had been entirely neglected experimentally.

To date, only CORA-33 and the SNL XR experiments have addressed the BWR "dry" core severe accident sequences.

2.2 XR TEST DESCRIPTION¹³

The ex-reactor (XR) experiments at SNL are designed to resolve phenomenological uncertainties concerning the behavior of relocating metallic melts draining into the lower regions of a dry BWR core as a result of a core-melt accident. The experiments are intended to determine under what conditions the metallic melts would form in-core blockages and under what conditions draining into the lower plenum would occur. The experiments specifically address the dry core accident conditions associated with depressurized BWR core melt accidents where rapid vessel blowdown has lowered the water level below the core plate. Under these conditions, the melt progression proceeds without the rapid oxidation-driven core damage mechanisms that have been more commonly investigated.

A major uncertainty currently exists with respect to the behavior of melting metallic core materials in the BWR under the dry core accident conditions associated with station blackout with vessel depressurization. At issue is the question of the formation of in-core metallic blockages in the lower region of the core, versus rapid draining of the relocating metallic components to the lower

plenum without the formation of an in-core blockage. The phenomenological uncertainty is important because of the potential impact upon the remainder of the accident, including influences upon the lower vessel head attack and the materials released following vessel failure.

The XR experiments will determine how melting and relocating metallic BWR core components accumulate in the lower region of the BWR core, and the interactions that occur with the core structures there. The degree of lateral melt spreading and flooding will be determined for a range of initial conditions, and the tendency of metallic melts to form blockages around the lower core structures and upon the core plate will be determined. Mechanisms of core plate attack and core plate bypass by the draining metallic melts will also be examined.

These phenomena will be investigated using prototypic materials and suitably scaled geometry so as to adequately represent a full-size *unit cell* within the BWR core lattice. In addition to Zircaloy-clad fuel rods, Zircaloy canister walls, and B₄C-filled stainless steel control blades, structures representative of the core plate, the lower fuel canister nose pieces, and the fuel support piece will be examined.

Metallic melts, representing the upper core region melting metallic components, will be prepared by means of inductive heating and will be transferred at a controlled rate into preheated test bundles representative of the lower 0.5 to 1 m of a dry BWR core. The initial experiments have addressed channel box and control blade behavior in response to accumulating metallic melts. Later experiments will incorporate all of the structural elements, including Zircaloy-clad UO₂ fuel rods. The end result of this experimental program will be an adequate understanding of the mechanisms associated with the transfer of molten core materials from the core region to the lower plenum region of the *dry-core* BWR core melt accident.

The general experimental approach used in the XR experiments is illustrated schematically in Figure 2.3. The test rig shown in Figure 2.3 includes the test bundle and melt generator (original design) situated within an enclosed confinement chamber. (A confinement chamber is necessary in order to inert the test environment with argon gas so that the heated test components will not react with air to form oxides or nitrides, and to prevent heated or molten Zircaloy used in the test from burning pyrophorically.) The test bundle will be preheated using both electrical resistive heating at the perimeter of the test bundle and convective heating supplied by a heated argon gas flow system.

In the original design, the melt generator was an inductively heated tilting type furnace (Figure 2.3) capable of preparing melts of up to about 100 kg of steel/Zircaloy mixture. The tilting mechanism would allow for a controlled rate of pour of the molten mixtures into the test bundle in order to simulate properly the time duration of the melt relocation. The molten material would be introduced into the test bundle using a ceramic funnel arrangement.

During February 1993, the tilting type furnace was tested via an inductive melt of stainless steel and then a controlled pour of the molten mass through a ceramic funnel into a catch tank. However, very little of the original melt mass (<25%) entered the catch tank. During the controlled pour, the high radiant heat losses from the melt caused rapid refreezing of the melt in

the tilt furnace pour spout and in the ceramic funnel. Thus it was demonstrated that this approach is not adequate and a new melt delivery system was designed.

The bottom discharge melter¹⁴ (shown schematically in Figure 2.4) is located on top of the test section so that the melt flows through an array of alumina tubes onto the desired structure; this unit is essentially an integral part of the test section. The bottom discharge melter has been tested successfully in May and June of 1993.

The test bundle designs to be investigated fall into two categories, as shown in Figure 2.5. The simpler design shown in the upper half of Figure 2.5 was employed in the initial tests. In the simpler design, only the channel box walls and the control blade structures are represented in the bundle cross section. The lateral dimensions allow a full 1/4 section of the cruciform-shaped BWR control blade to be included in the design, and preserve the proportion of "bladed" interchannel gap to "un-bladed" gap.

The more complicated test design shown in the lower half of Figure 2.5 includes an array of 72 Zircaloy-clad UO₂ fuel rods, in addition to the channel box and control blade structures. These tests will investigate flooding effects in the fuel canister region that occur when melts intrude into the fuel canisters. Fuel rod grid spacers and a tie plate/nose piece structure will be included in the base of this design, in addition to the core plate structure. This will allow investigation of the flooding phenomena occurring within the fuel canister and the potential drainage paths through the fuel nose piece, bypassing the core plate. The large rod array will make use of the heated argon gas flow system in order to preheat the fuel rods. In addition, the perimeter region can be electrically heated in order to minimize radial conductive heat losses through the perimeter insulation.

The principal on-line diagnostic to be used in the XR experiments is thermocouple instrumentation. There is also a real-time x-ray imaging device¹⁵ (see Figure 2.6) to observe the melt relocation within the test section.

Two XR experiments have been completed, both utilizing the simpler design shown in the upper half of Figure 2.5. The XR1-1 test was successfully executed on July 23, 1993.¹⁶ The XR1-2 experiment was completed on November 5, 1993.¹⁷

2.3 PEER REVIEW COMMENTS ON THE EX-REACTOR EXPERIMENTS

In 1993, the USNRC convened an expert technical review group to help guide the future course of NRC research in the late phase melt progression area; specifically, this group was to review the ex-reactor and late phase experiments at SNL and the late-phase DEBRIS porous media modeling effort¹⁸⁻¹⁹ at SNL. Over a three day period in January 1994 (Rockville, Maryland), the SNL researchers presented papers on the results and posttest analyses of completed tests and the planning, purpose, and supporting pretest analyses for proposed new experiments. During this meeting, the group members were instructed to provide a summary assessment of the ex-reactor program and an assessment of the late phase melt progression information that was presented at the meeting.

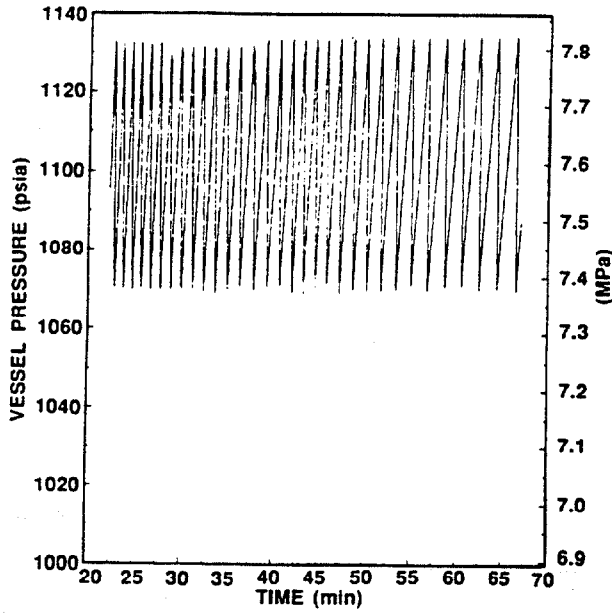
With respect to the SNL ex-reactor experiments, the review group unanimously recommended proceeding with the XR2 series of tests. Also, it was recommended that the planning for the XR2 experiments be augmented by a firm, documented, analytical basis for the debris pour compositions, rates, and distributions as well as for the initial temperatures of the core plate and overlying structures that will receive the pours. It was also suggested that a best-estimate simulation of a BWR dry-core accident scenario be performed (using SCDAP/RELAP5) to supply the desired initial and boundary conditions for the XR2 tests.

2.4 ORNL SUPPORT OF THE XR2 TEST SERIES

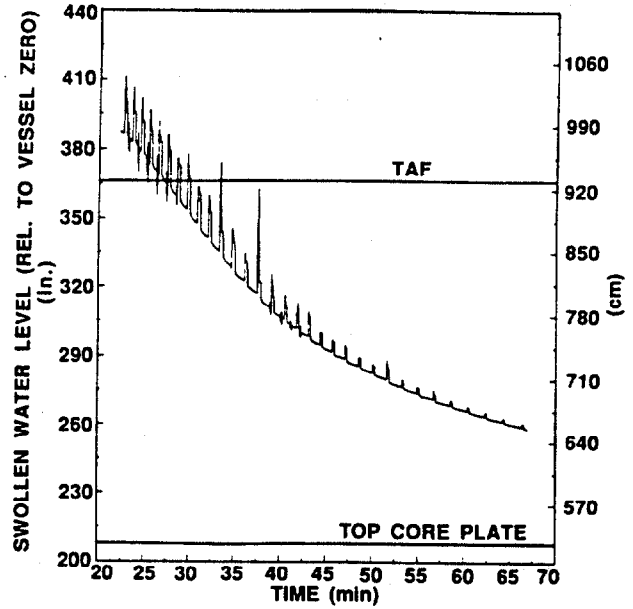
In response to the peer review recommendations for the SNL XR2 series of experiments, Task 5 of JCN W6202 for the BEAMD Program was modified to authorize a best-estimate analysis of a BWR dry-core severe accident sequence using the SCDAP/RELAP5 code.

Chapter 3 describes the SCDAP/RELAP5 model employed in the ORNL analysis; Chapter 4 presents the results of the ORNL analysis.

- LOSS OF INJECTION AFTER BATTERY FAILURE
- LOSS OF ABILITY TO MANUALLY MANIPULATE SAFETY RELIEF VALVES (SRVs)
- PRESSURE DEPENDENT ON SRV AUTOMATIC ACTUATIONS



- BOILOFF



- CORE STEAMING DOMINATED BY SRV ACTUATIONS

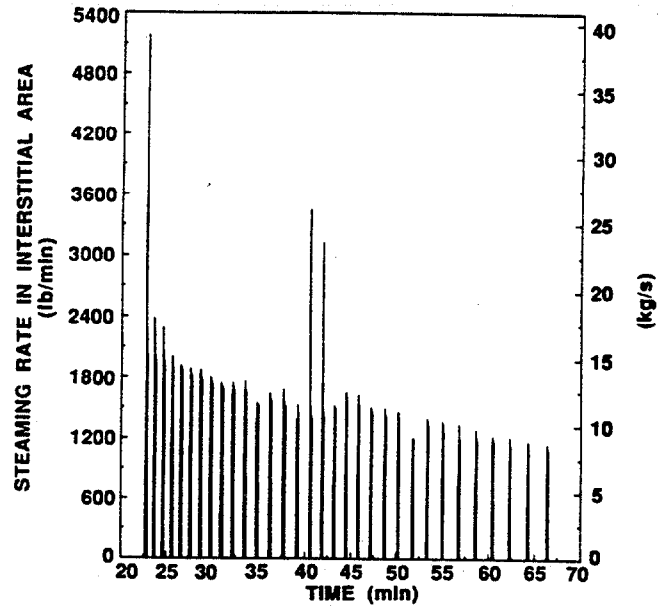
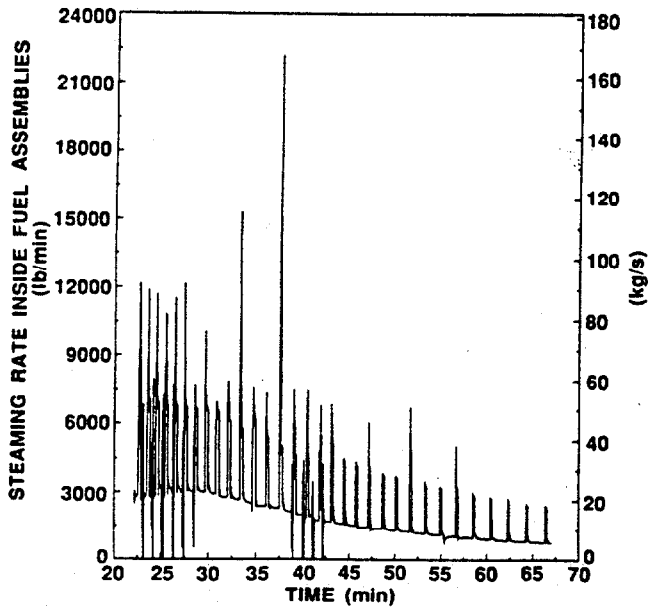
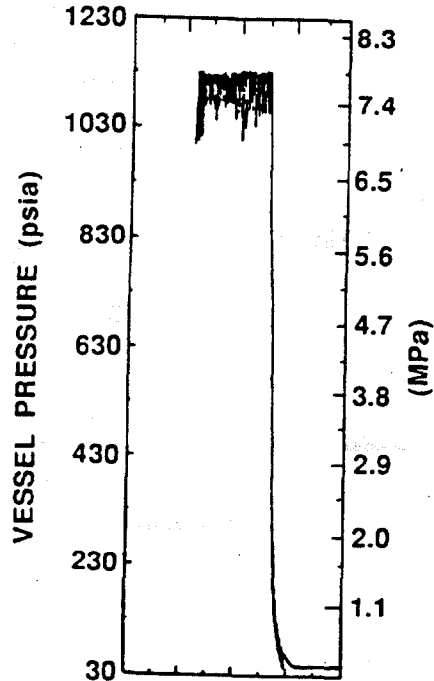


Figure 2.1. Characteristics of a BWR long-term station blackout accident sequence.

- NO INJECTION
- VESSEL DEPRESSURIZED



- BOILOFF WITH FLASHING DURING DEPRESSURIZATION
- STEAM-STARVED CORE DEGRADATION

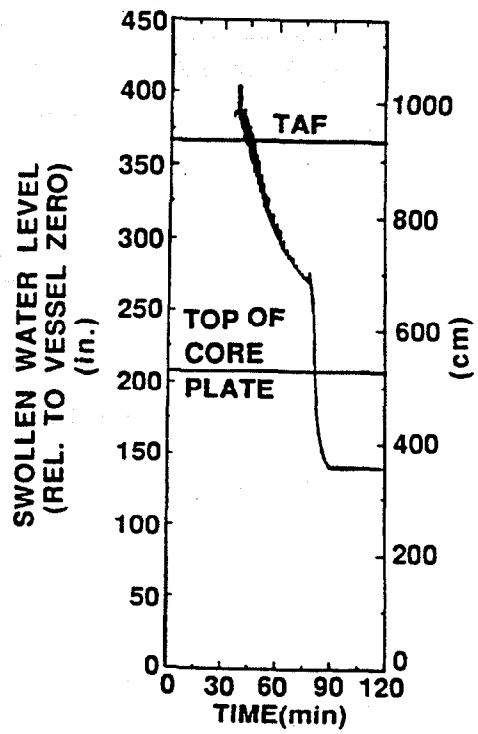


Figure 2.2. Characteristics of a BWR short-term station blackout accident sequence.

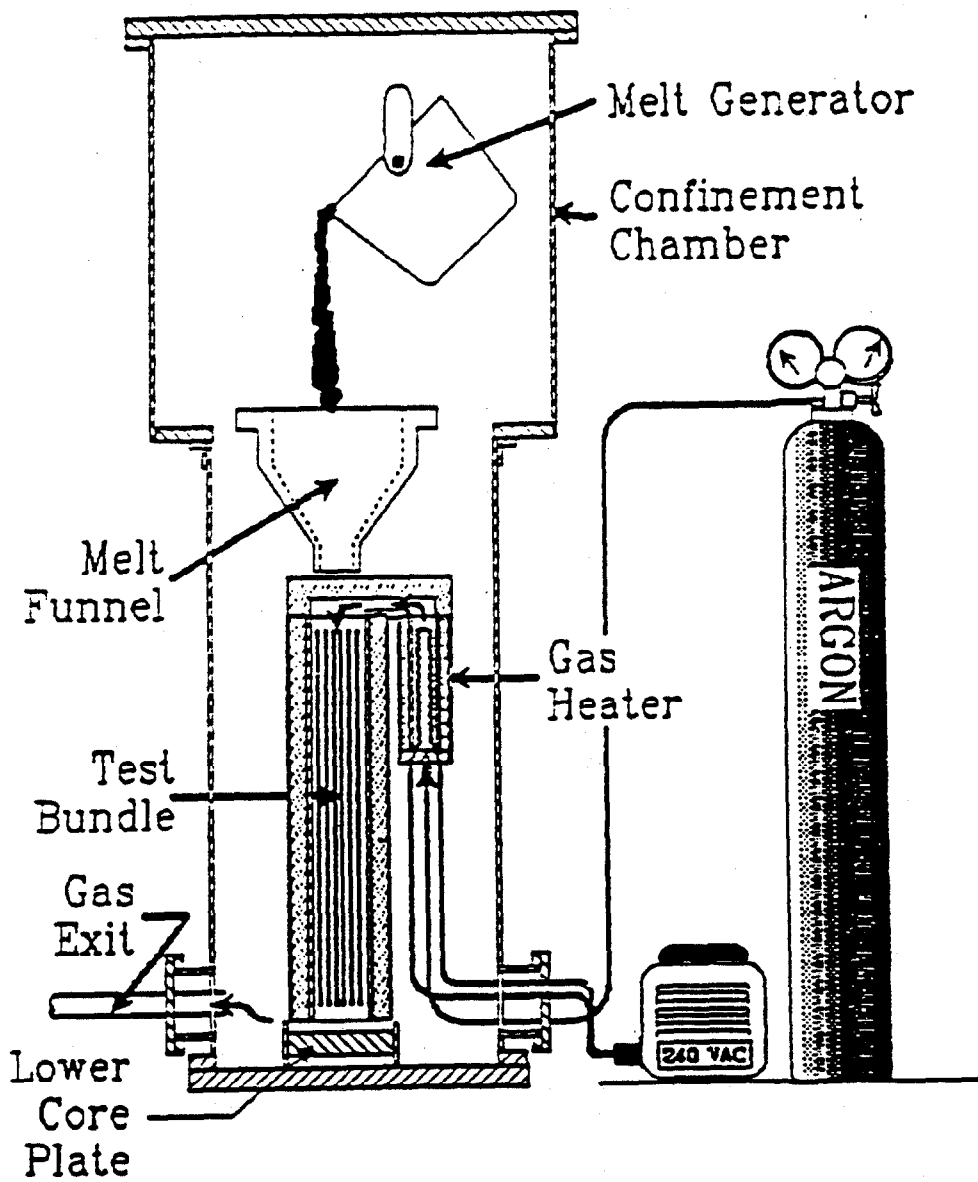


Figure 2.3. Schematic diagram showing the general experiment approach to be used in the conduct of the XR experiments (Reference 13).

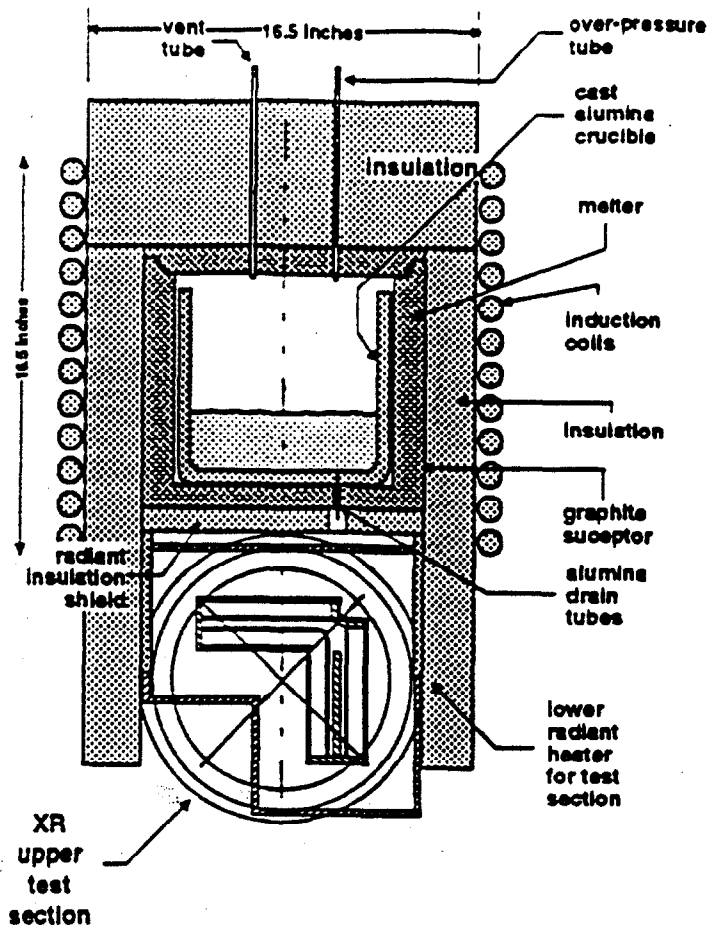
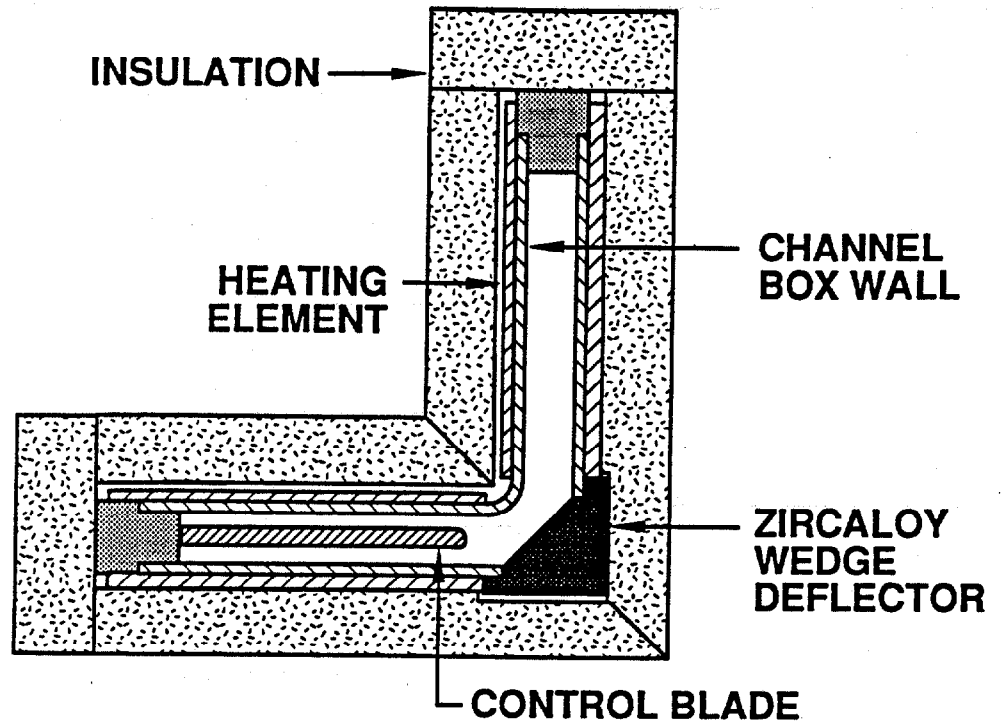


Figure 2.4. XR bottom-pour melter with the upper test section shown rotated 90° (Reference 14).

XR Series 1



XR Series 2

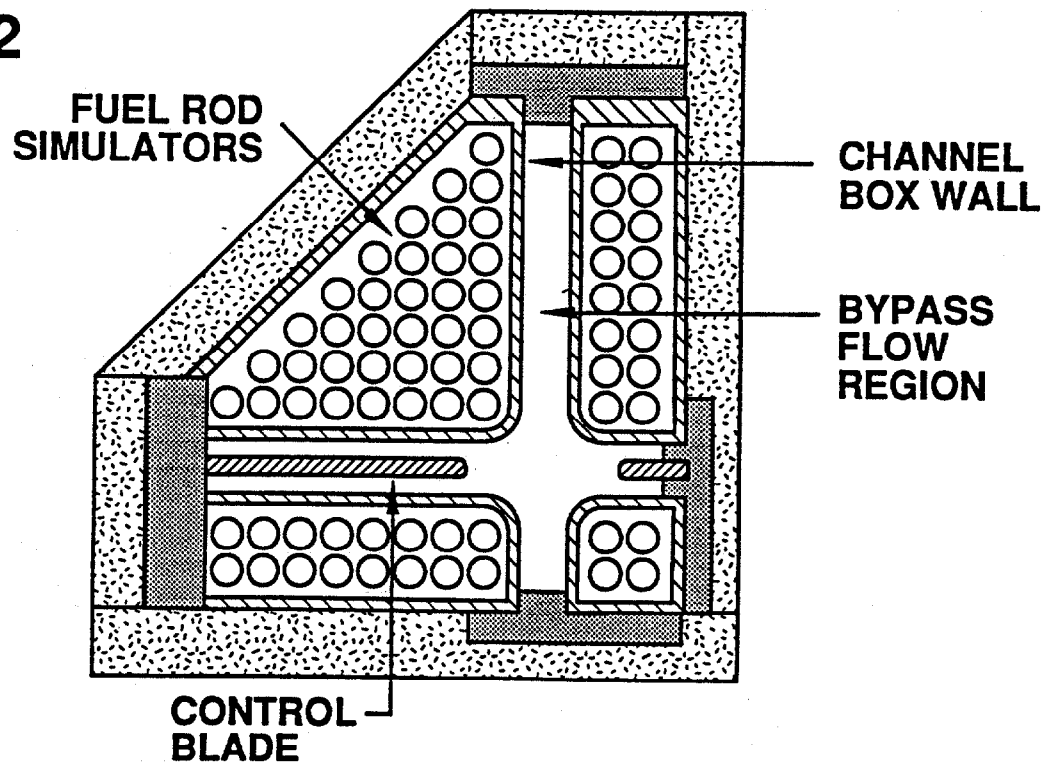


Figure 2.5. Cross-sectional views of two test bundle designs to be investigated in the XR experiments (Reference 13).

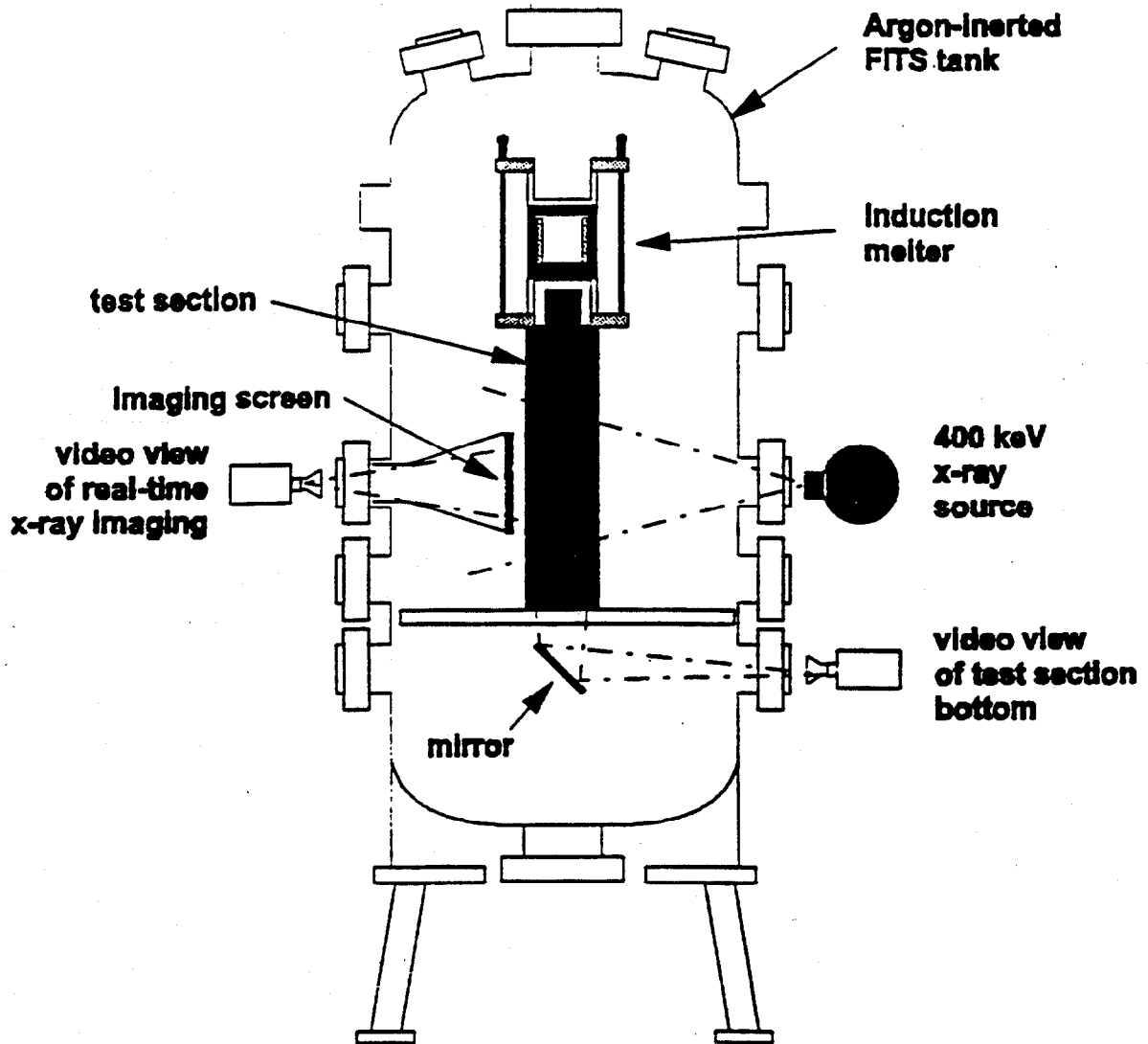


Figure 2.6. Schematic of the XR test facility (Reference 15).

3. SCDAP/RELAP5 MODEL FOR BROWNS FERRY

A SCDAP/RELAP5 model has been developed for the Browns Ferry Nuclear Plant design based upon a short-term station blackout (STSB) accident sequence. This STSB model was developed by modifying a Browns Ferry input deck representing a large-break loss of coolant accident (LOCA) sequence obtained from INEL. Other improvements were made to incorporate more detailed axial and radial power profiles and to refine the representation of the structures in the lower core, core-plate region, and lower plenum.

3.1 DESCRIPTION OF BASIC MODEL

3.1.1 Hydrodynamic Nodalization

A nodalization diagram for the Browns Ferry reactor vessel and associated piping is shown in Figure 3.1. The reactor coolant system is represented from the feedwater inlet to the turbine inlet and includes the reactor pressure vessel, two recirculation loops, the feedwater piping, the control rod drive (CRD) cooling water, and the steam piping. The recirculation loop on the left-hand side of Figure 3.1 was originally used at INEL to represent a LOCA sequence. For the STSB accident sequence, both recirculation loops remain intact (i.e., the valves between volumes 200 and 998 and volumes 210 and 999 are closed). The Browns Ferry containment is not represented explicitly. Rather, the safety/relief valves (SRVs) discharge into volume 561, which is assumed to remain at a constant pressure of 45 psia.

A more detailed nodalization diagram of the lower half of the reactor pressure vessel is shown in Figure 3.2 with hydrodynamic volumes represented by open boxes and solid structures represented by shaded boxes. The active core is divided into four radial rings and thirteen axial nodes. The center ring of the core (right-hand side of Figure 3.2) represents ~55% of the fuel bundles, while the other three rings near the periphery of the core (where the power density is greatly reduced) each represent ~15% of the fuel bundles. The lower 1.07 m (3.5 ft) of the active core (which is the region of interest to the XR experiments) is divided into 7 axial nodes, while the upper 2.74 m (9.0 ft) of the active core is divided into 6 axial nodes.

In each of the four radial rings, there is one pipe volume that represents the coolant flow inside the fuel assemblies (volumes 320, 321, 322, and 323) and one pipe volume that represents the coolant flow outside the fuel assemblies in the interstitial region surrounding the control blades (volumes 370, 324, 325, and 326). The interstitial volumes outside the fuel assemblies are connected by cross-flow junctions that allow coolant to flow horizontally between the center and the periphery of the core.

The primary coolant flow through the core (about 90% of total) is from the lower plenum (volumes 292, 293, and 294) through the fuel support pieces and lower tie plates (volumes 300, 301, 302, and 303) and into the fuel assemblies. The remaining core coolant flow (about 10% of total) is through the interstitial region. Coolant enters the interstitial region by either flowing

through holes machined in the lower tie plates, leaking past the core plate, or flowing through the control rod guide tubes (volumes 340 and 350) from the CRD cooling water pumps.

The jet pumps are represented by volumes 260, 265, and 270 (first recirculation loop) and volumes 261, 266, and 271 (second recirculation loop). In a BWR, the upper mixing sections of the jet pumps are connected to the lower diffuser sections by mechanical slip fits for easy removal during maintenance. The leakage through these slip joints is represented by junctions that connect the jet pumps (bottom of volumes 265 and 266) to the annulus region (volume 455).

3.1.2 Structure Models

The fuel rods, water rods, and BWR control blade/channel boxes are represented by SCDAP components that include the effects of oxidation, melting, and relocation. RELAP5 heat structures (which do not model oxidation and melting) are used to represent the other structures, including: (1) the lower tie plates, (2) the fuel support pieces, (3) the core plate, (4) the core plate stiffeners, (5) the core shroud, (6) the control rod guide tubes and CRD housings, and (7) the reactor pressure vessel wall.

The SCDAP components are shown in Figure 3.2 as shaded boxes and are labeled with numbers 1 through 12. A summary of these SCDAP components is provided in Table 3.1. All fuel rods, water rods, and control blade/channel boxes within each core radial ring are represented by single representative SCDAP components. The SCDAP components transfer heat by convection with the adjacent hydrodynamic volumes and by radiation (radial direction only) with other adjacent SCDAP components.

The RELAP5 heat structures are identified in Figure 3.2 with 4-digit numbers. Figure 3.3 shows a more detailed diagram of the RELAP5 heat structures in the core plate region. A summary of these RELAP5 heat structures is provided in Table 3.2. The RELAP5 heat structures transfer heat by convection with the adjacent hydrodynamic volumes, but there is no calculated radiative heat transfer between RELAP5 heat structures or between RELAP5 heat structures and SCDAP components.

3.1.3 Decay Power Distribution

Detailed 3-D core power data was developed by EPRI (4/2/87) for the Susquehanna nuclear power plant equilibrium core at the end of cycle (10.5 GWD/MTU). This data provides the nuclear heat generation at 25 axial elevations for each of the 764 8x8 fuel assemblies. Because the Susquehanna core configuration is identical to the Browns Ferry core configuration, this power data was applied to the Browns Ferry STSB simulation.

Based on the thirteen core axial nodes shown in Figure 3.2 (and the core nodalization discussed in Section 3.1.1), the Browns Ferry power profiles were calculated from the Susquehanna data. The calculated radial and axial power profiles are shown in Figures 3.4 and 3.5, respectively. Note that the peripheral fuel assemblies produce only one third the power as the center fuel assemblies. Also note that the peak power in the center fuel assemblies is at a low elevation in the core.

The RELAP5 point kinetics model is used to predict the decay power after scram. When default input parameters are used, the RELAP5 point kinetics model predicts decay heat generation that is too large when compared with the realistic decay heat profiles described in NUREG/CR-4169.²⁰ To compensate, a fission product yield factor of 0.81 (instead of the default 1.0) is used in the RELAP5 point kinetics model to reduce the predicted decay power in accordance with NUREG/CR-4169.

3.1.4 STSB Accident Sequence

In the Browns Ferry STSB model, the first 300 s (5 min) of the simulation represents a period of steady-state operation of the reactor at full power (3293 MWt). The STSB accident sequence is caused by a loss of offsite AC power and is initiated at 300 s in the SCDAP/RELAP5 input deck by: (1) loss of AC power to the recirculation pumps, (2) loss of AC power to the CRD cooling water pumps, (3) initiation of MSIV closure, (4) initiation of scram, and (5) loss of the turbine-driven feedwater pumps and initiation of feedwater coast-down. Throughout the duration of the STSB accident sequence, all sources of cooling water for the core are unavailable.

The recirculation pumps are modeled explicitly using RELAP5 pump components that include the effect of the inertia of the motor and impeller. The recirculation pumps continue to rotate in response to coolant flow through the pumps even though there is no power input to the shafts after 300 s. The CRD cooling water pumps are not modeled explicitly and the relatively small CRD cooling water flow is simply set to zero at 300 s.

The MSIV closure time and the control blade insertion time during scram is modeled in the Browns Ferry STSB simulation. The MSIVs begin to close at 300 s and are fully closed by 305 s. After the scram signal at 300 s, the control blades begin to move at 300.2 s and are fully inserted into the core by 302.8 s. In the RELAP5 point kinetics model, an appropriate amount of negative reactivity is associated with this insertion of the control blades into the core.

After the feedwater trip signal at 300 s, the turbine-driven feedwater pumps briefly continue to supply coolant to the vessel. Data available at ORNL from actual tests conducted at the Susquehanna power plant (with similar feed pumps) were used to determine the declining amount of feedwater during the pump coast-down. This Susquehanna data and the feedwater coast-down representation used in the SCDAP/RELAP5 model are shown in Figure 3.6. In the STSB simulation, the feedwater flow continues at 100% for 11.78 s after the trip signal and then reduces linearly to zero by 35 s after the trip signal. The total amount of coolant injected during the feedwater pump coast-down is 86,660 lbm, which is about 14% of the normal vessel inventory.

The SCDAP/RELAP5 model represents automatic actuation of the SRVs during the initial slow boil-off; manual operation of the SRVs by reactor operators as specified in the Emergency Procedure Guidelines is not represented during this time period. The individual SRVs open and close at different pressures. The first SRV opens when the vessel pressure reaches 1115 psia (other SRVs may also open if the pressure continues to increase) and remains open until the vessel pressure has declined to 1014 psia.

Manual actuation of the Automatic Depressurization System (ADS) as specified in the Emergency Procedure Guidelines is represented in the SCDAP/RELAP5 model by opening the ADS associated SRVs when the collapsed water level in the fuel assemblies in the center ring of the core reaches one third core height.

3.2 MODEL TO REPRESENT FUEL BUNDLE TEMPERATURE DISTRIBUTION

An additional and more detailed SCDAP/RELAP5 model of Browns Ferry has been developed to represent the effects of the local temperature distribution within the central region fuel bundles. In the basic model of Browns Ferry described in Section 3.1, all fuel rods within each core radial ring are represented by a single representative SCDAP fuel rod component. The more detailed model represents the fuel rods in the center radial ring with three SCDAP fuel rod components. These components are arranged as shown in Figure 3.7 so as to predict the temperature distribution within the 62 fuel rods: component 10 represents the 34 fuel rods at the middle of each bundle, component 11 represents the 13 fuel rods in the outer rows adjacent to a control blade, and component 12 represents the 15 fuel rods in the outer rows not adjacent to a control blade.

A summary of the SCDAP components for the more detailed model with the center assemblies represented by three fuel rod groups is provided in Table 3.3. A comparison of Tables 3.1 and 3.3 reveals that the basic and the more detailed SCDAP/RELAP5 models are identical except for the level of detail used to model the fuel rods in the assemblies at the center of the core (ring 1). In the remainder of this report, the model described in Section 3.1 will be referred to as either the "basic model" or the "model with one fuel rod group" and the model defined in this Section will be referred to as either the "more detailed model" or the "model with three fuel rod groups."

In the more detailed model, the three fuel rod groups in the center core radial ring interact with a single RELAP5 pipe volume (number 323) that provides a common sink temperature for convection heat transfer. During the early phases of the STSB accident simulation when this volume is filled with water and there is no radiation heat transfer, the temperature predictions for the three fuel rod groups are identical. Later in the simulation after the water has drained from this volume, radiation heat transfer causes the temperature predictions for the three fuel rod groups to progressively differ. The view factors used in the input deck for radiation between the three fuel rod groups, the water rods, and the channel boxes were calculated using the VIEW²¹⁻²² code developed by NASA.

3.3 MODEL VERIFICATION

To verify the Browns Ferry SCDAP/RELAP5 input deck, two types of testing have been conducted. First, calculations representing steady-state operation of the reactor at full power (3293 MWt) were performed and compared with the specifications provided in the Browns Ferry Final Safety Analysis Report (FSAR). Second, the SCDAP/RELAP5 transient predictions for the STSB accident sequence were compared with predictions from the BWR-LTAS²³/BWRSAR¹ codes developed previously at ORNL. During this verification testing, several adjustments were made to parameters in the SCDAP/RELAP5 input deck (such as flow loss coefficients) to improve the Browns Ferry simulation. Also, several minor errors in the input deck were discovered and corrected (these have been reported to the INEL staff that maintain this deck).

The results of the steady-state calculation are shown in Table 3.4. The feedwater and steam flow rates predicted by SCDAP/RELAP5 are about 1% less than the FSAR values. The predicted recirculation flow rate (i.e., the combined flow rate through both recirculation loops in Figure 3.1) is identical to the FSAR specification, which indicates that the flow losses through the core and the remainder of the reactor vessel are being modeled correctly within SCDAP/RELAP5. The predicted flow rate through the interstitial region is about 10% of the total flow rate through the core. In a typical BWR, this ratio of interstitial to total core flow is between 10% and 12%, depending on the age of the fuel assemblies.

A comparison of the SCDAP/RELAP5 and BWR-LTAS/BWRSAR predictions for the STSB accident sequence is shown in Table 3.5. This Table lists the timing of important events that occur during the boil-off and early core degradation phases of the accident. There is excellent agreement between SCDAP/RELAP5 and BWR-LTAS/BWRSAR through the time of ADS actuation. Nevertheless, because the control blade and channel box melting models in BWR-LTAS/BWRSAR are less detailed than those now available in SCDAP/RELAP5, some differences exist in the predicted timing of these events.

Table 3.1. Summary of SCDAP components for basic model

Number	Type	Description
1	Fuel rod	100 fuel assemblies at periphery of core (ring 4)
2	Water rod	100 fuel assemblies at periphery of core (ring 4)
3	Control blade/channel box	19 control blades at periphery of core (ring 4)
4	Fuel rod	128 fuel assemblies (ring 3)
5	Water rod	128 fuel assemblies (ring 3)
6	Control blade/channel box	32 control blades (ring 3)
7	Fuel rod	104 fuel assemblies (ring 2)
8	Water rod	104 fuel assemblies (ring 2)
9	Control blade/channel box	26 control blades (ring 2)
10	Fuel rod	432 fuel assemblies at center of core (ring 1)
11	Water rod	432 fuel assemblies at center of core (ring 1)
12	Control blade/channel box	108 control blades at center of core (ring 1)

Table 3.2. Summary of RELAP5 heat structures in the lower vessel

Number	Description
2921, 4351	Reactor pressure vessel
2701, 2711	Jet pumps
4501	Middle core shroud
2931, 4751	Lower core shroud
2941, 3401	Control rod guide tubes and CRD housings
2942	Core plate stiffener plates and rods
2943	Core plate
3001	Fuel support pieces and lower tie plates at periphery of core (ring 4)
3011	Fuel support pieces and lower tie plates (ring 3)
3021	Fuel support pieces and lower tie plates (ring 2)
3031	Fuel support pieces and lower tie plates at center of core (ring 1)

Table 3.3. Summary of SCDAP components for model with 3 fuel groups

Number	Type	Description
1	Fuel rod	100 fuel assemblies at periphery of core (ring 4)
2	Water rod	100 fuel assemblies at periphery of core (ring 4)
3	Control blade/channel box	19 control blades at periphery of core (ring 4)
4	Fuel rod	128 fuel assemblies (ring 3)
5	Water rod	128 fuel assemblies (ring 3)
6	Control blade/channel box	32 control blades (ring 3)
7	Fuel rod	104 fuel assemblies (ring 2)
8	Water rod	104 fuel assemblies (ring 2)
9	Control blade/channel box	26 control blades (ring 2)
10	Fuel rod	34 fuel rods at center of bundle in 432 fuel assemblies at center of core (ring 1)
11	Fuel rod	13 fuel rods at edge of bundle adjacent to control blade in 432 fuel assemblies at center of core (ring 1)
12	Fuel rod	15 fuel rods at edge of bundle not adjacent to control blade in 432 fuel assemblies at center of core (ring 1)
13	Water rod	432 fuel assemblies at center of core (ring 1)
14	Control blade/channel box	108 control blades at center of core (ring 1)

Table 3.4. SCDAP/RELAP5 predictions for steady-state operation at full power

Parameter	SCDAP/RELAP5	FSAR
Nuclear heat generation, Mwt	3293 ^a	3293
Feedwater flow, Mlbm/h	13.20	13.33
CRD cooling water flow, Mlbm/h	0.03 ^a	0.05
Steam flow, Mlbm/h	13.23	13.38
Recirculation flow, Mlbm/h	34.2	34.2
Flow through fuel assemblies, Mlbm/h	92.2	not available
Flow through interstitial region, Mlbm/h	10.3	not available
Total flow through core, Mlbm/h	102.5 ^a	102.5

^aParameter is specified directly in the SCDAP/RELAP5 input deck.

Table 3.5. Comparison of SCDAP/RELAP5 and BWR-LTAS/BWRSAR predictions

Event	Time After Scram (min)		
	SCDAP/RELAP5 (1 fuel rod group)	SCDAP/RELAP5 (3 fuel rod groups)	BWR-LTAS/BWRSAR (2 fuel rod groups)
Downcomer collapsed level at top of active fuel	56.8	56.8	55.2
ADS actuation (core collapsed level at 1/3 active fuel)	91.3	91.6	91.1
First control blade liquefaction	125.0	125.2	131.0
First interstitial blockage between control blade and channel box	127.6	127.9	not applicable
First channel box liquefaction (Zr/SS eutectic)	132.5	132.7	not applicable
First channel box melting (pure Zr)	139.6	140.8	132.6

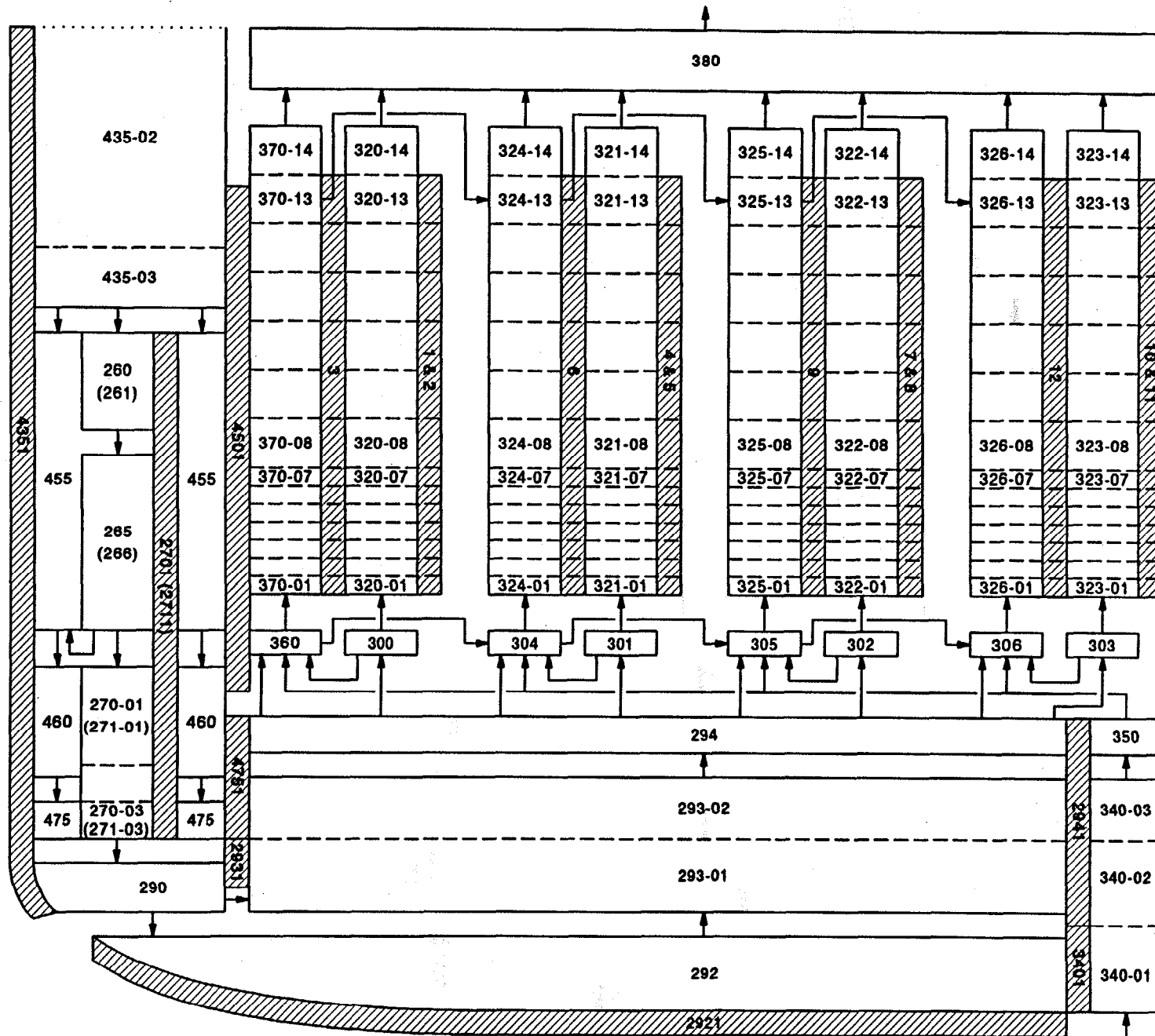


Figure 3.2. Nodalization diagram of lower reactor vessel.

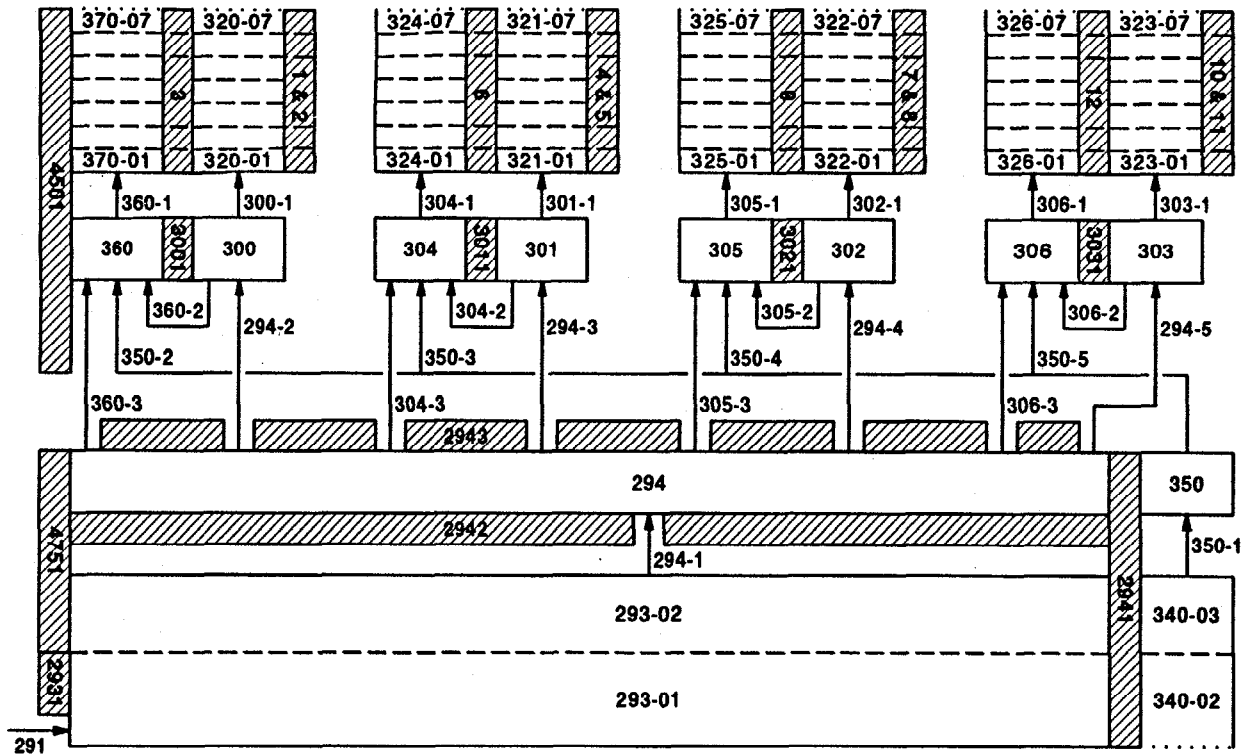


Figure 3.3. Nodalization diagram of core plate region.

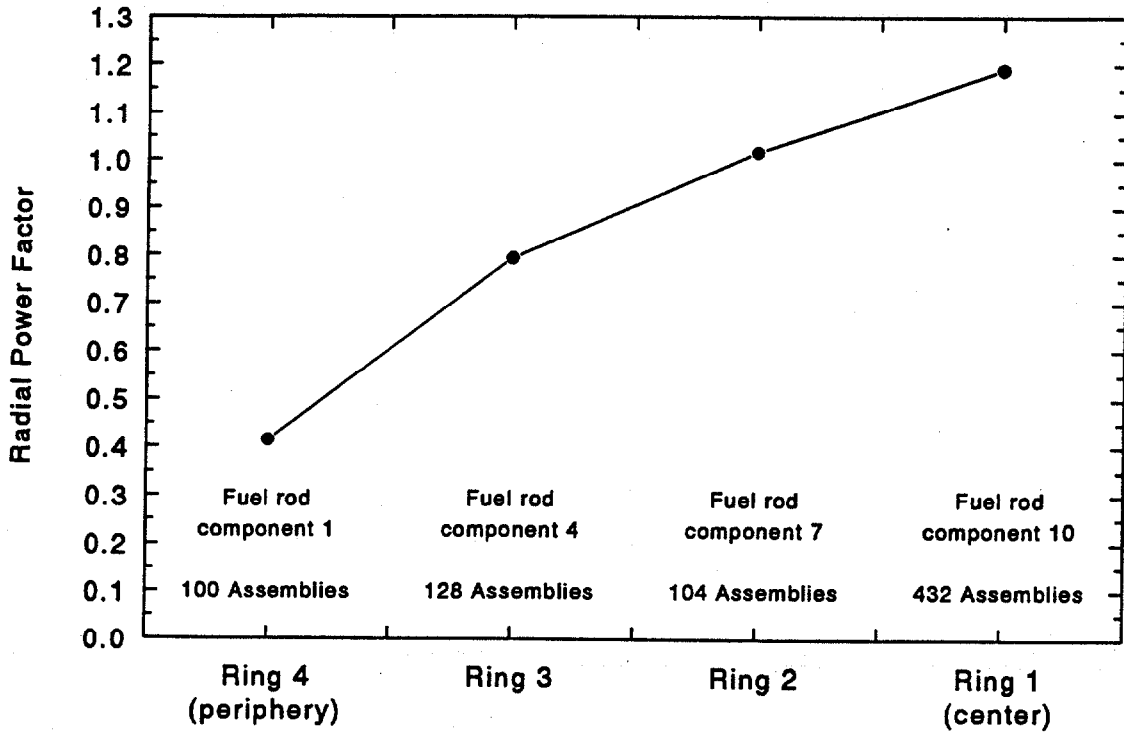


Figure 3.4. Browns Ferry power profile for 4 radial rings.

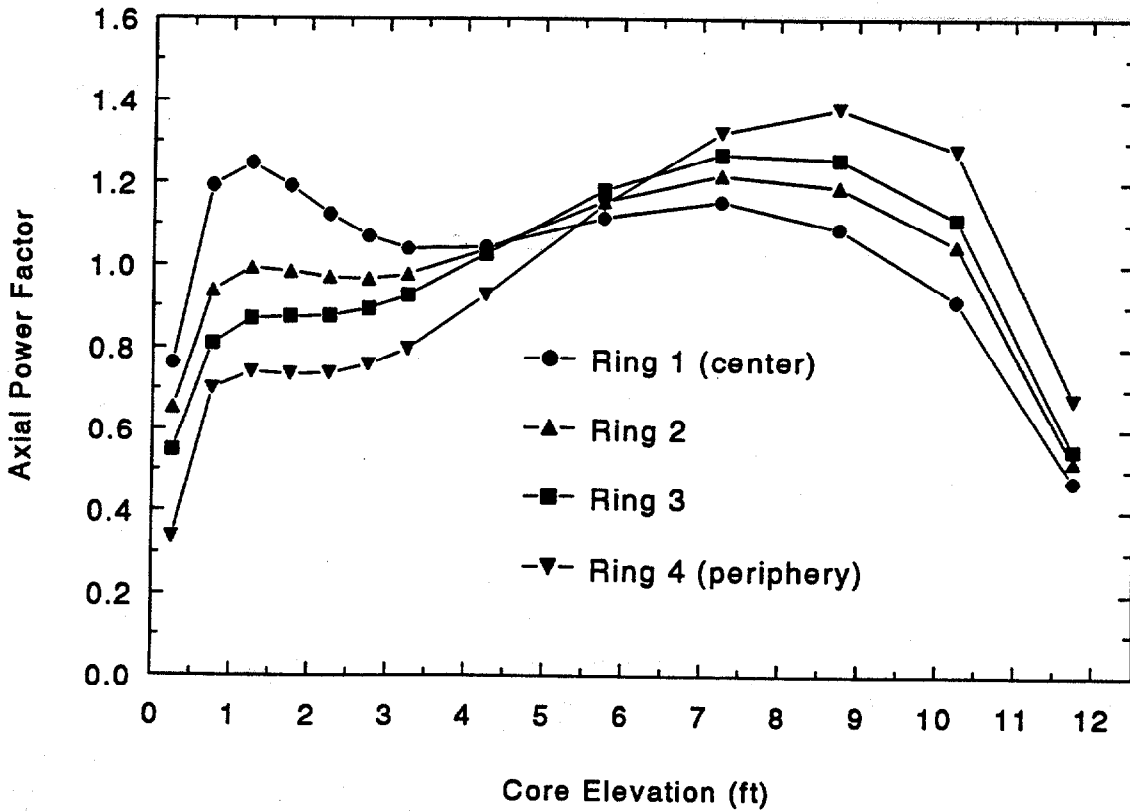


Figure 3.5. Browns Ferry power profiles for 13 axial nodes.

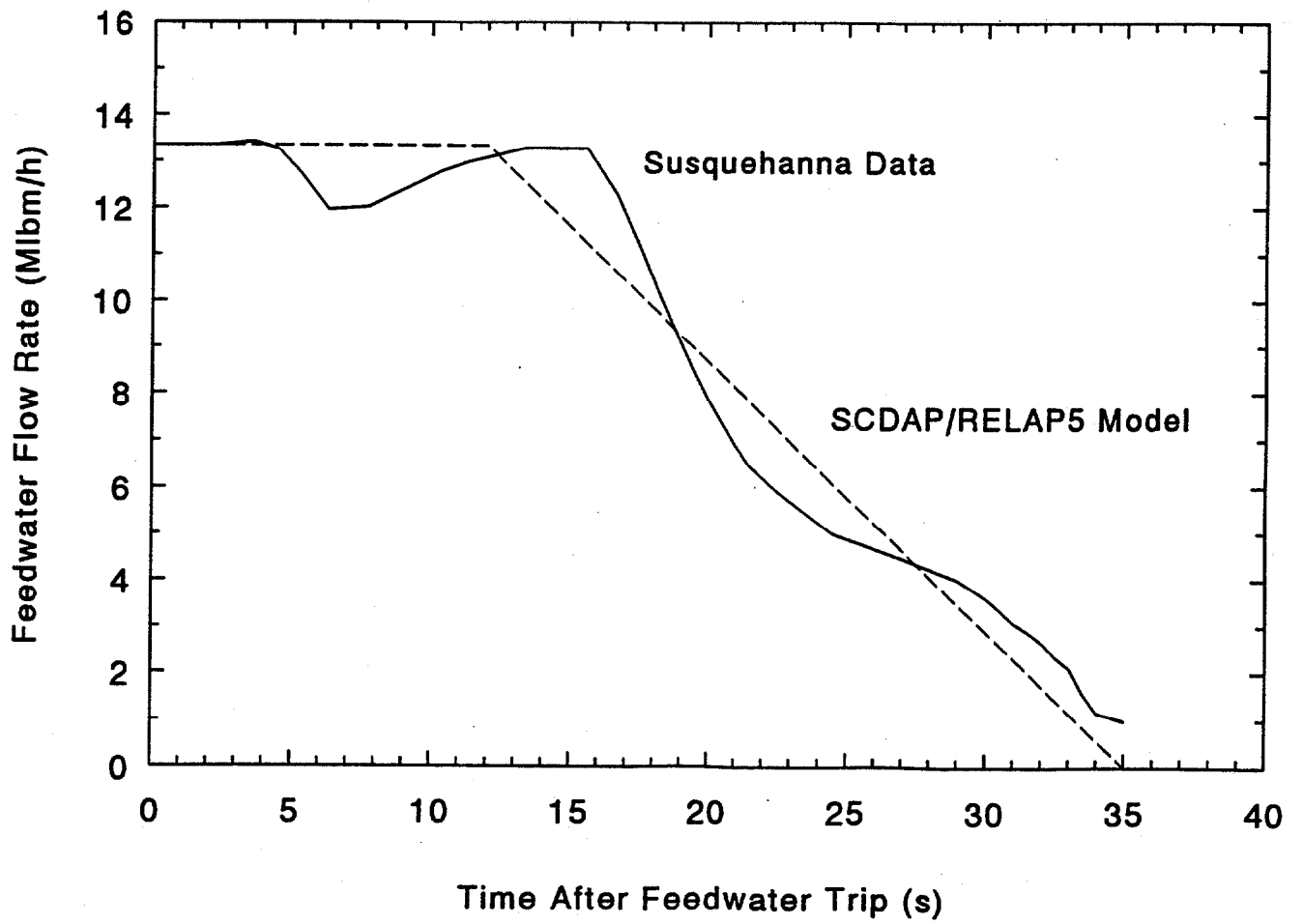


Figure 3.6. Feedwater coast-down representation.

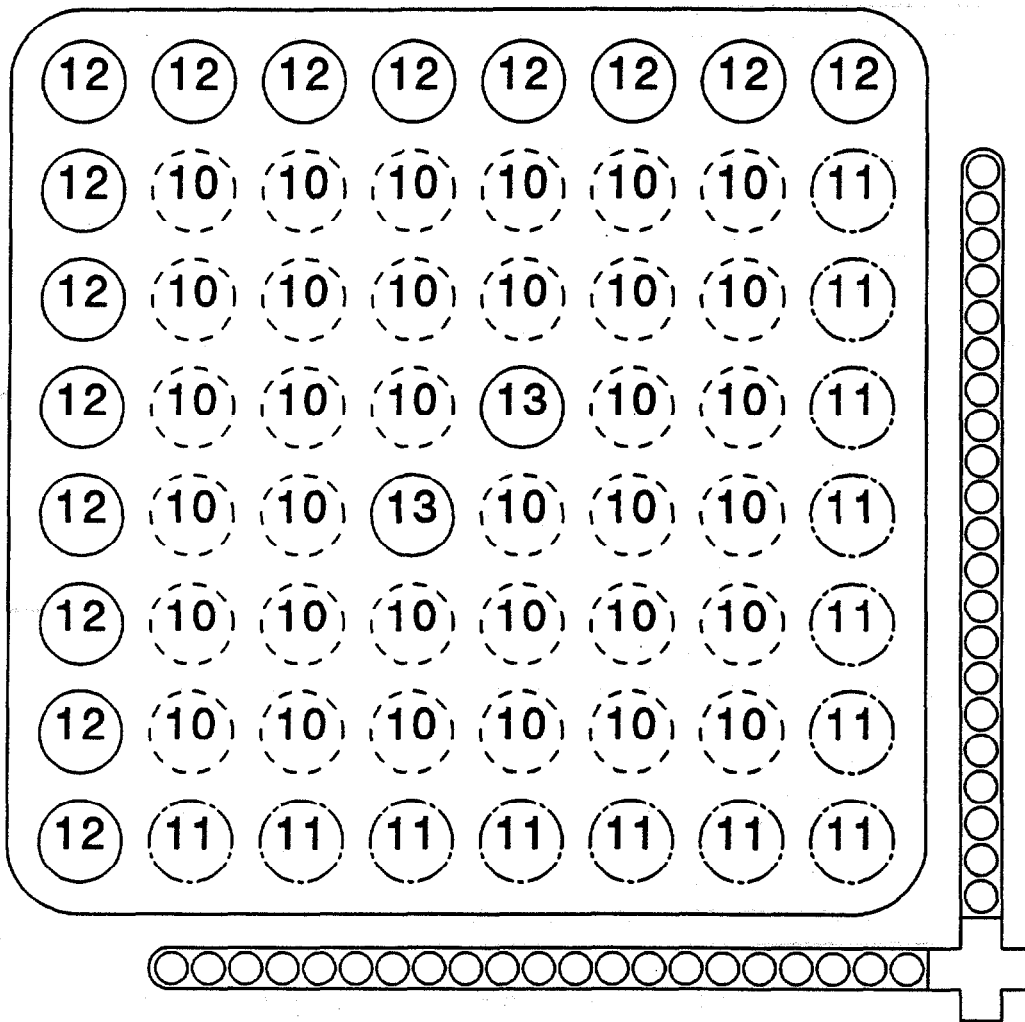


Figure 3.7. Center assemblies represented by three fuel rod groups.

4. INITIAL AND BOUNDARY CONDITIONS FOR THE XR2 TESTS

The objective of the best estimate simulation of the Browns Ferry STSB accident sequence using SCDAP/RELAP5 is the development of initial and boundary conditions for the XR2 series of tests. The initial conditions are the thermal state of the coreplate, bundle nosepieces, and lower 0.5-1.0m of the core at the time of incipient liquefaction of the control blades in the central region of the core. The boundary conditions consist of the debris pour compositions, rates, and distributions from the upper core into the lower core region.

Section 4.1 discusses the STSB transient. Section 4.2 presents the initial thermal condition of the lower core at incipient control blade liquefaction. Section 4.3 gives the melt relocation rates, compositions, and distribution into the lower core for a period of approximately 3000s after initial control blade liquefaction.

4.1 BROWNS FERRY STSB TRANSIENT

The Browns Ferry STSB accident sequence simulation is described in Section 3.1.4. The results from the "model with three fuel rod groups" will be discussed; referring to Table 3.5, there is very little difference in the event timing predicted by the "model with one fuel rod group" and the more detailed "model with three fuel rod groups."

The predicted response of the reactor vessel pressure is illustrated in Figure 4.1; note that there are two time scales. The lower "SCDAP/RELAP5" time scale includes an initial 300s of steady-state full power operation while the upper scale provides time after scram (the following discussion is based upon this time after scram). The vessel pressure rides on the SRV actuations until the ADS is manually initiated, which occurs when the in-core water level (Figure 4.2) reaches 1/3 of the active core height. The vessel depressurizes until it equilibrates with the containment pressure.

The vessel water inventory flashes during the depressurization, stabilizing in the lower plenum (see Figure 4.2) at a level of 345 cm (136 in) above the bottom of the vessel. This is 182 cm below the top of the coreplate; thus the core region is dry. The lower plenum water level is 28 cm above the shroud bottom baffle and the discharge of the jet pumps; therefore a gross gaseous natural circulation loop (annulus-lower plenum-core-upper plenum-annulus) does not occur. Localized gas natural circulation loops from the intersitial region of the core to the volume just below the core plate and then into the fuel assemblies (and also in the reverse direction) are predicted to exist. However, the steam generation rate in the lower plenum is low, and therefore very little steam is available for metal/steam oxidation reactions in the core. Significant hydrogen production starts at approximately 106 min. At 175 min after scram, only 90 kg of hydrogen has been generated (see Figure 4.3).

As shown in Figure 4.4, the "steam cooling maneuver" does temporarily cool the core (by nearly 250 K) and delays the heatup by 12-13 min.

The first control blade liquefaction is predicted to occur at 125.2 min in the center of the core at axial node 5 (61-76.2 cm above the bottom of the active fuel [BAF]).

The timing of these events is confirmed by an independent calculation using the BWR-LTAS/BWRSAR code suite (see Table 3.5).

4.2 INITIAL THERMAL CONDITIONS

When control blade material begins to relocate into the lower core at 125.2 min, the detailed SCDAP/RELAP5 simulation with three fuel rod groups predicts the temperatures given in Table 4.1 for the structures below the 61 cm level (relative to BAF). A guide to the core structures addressed in Table 4.1 is given in Figure 4.5.

Transient plots of the thermal response of these lower core structures from 123 to 126 min are presented in Figures 4.6-4.10. The structural thermal response in node 4 (Figure 4.10) to relocating melt is small since the control blade is within 30 K of the control blade liquefaction temperature and there is little heat transfer from the melt to the underlying solid blade. However, in node 3 (Figure 4.9) the refreezing melt strongly influences the structural thermal responses.

The detailed SCDAP/RELAP5 model was developed specifically to address the temperature distribution within a fuel bundle at an axial plane. The temperatures in Table 4.1 and Figures 4.6-4.10 are generated from this detailed model. Table 4.2 contains the structural temperature differences within the fuel assembly for nodes 1-4 at 125.2 min (this Table was generated from Table 4.1).

The maximum temperature difference within the fuel assembly at an axial plane in the lower 61 cm of the core is 20 K (node 4 in Table 4.2). Given this difference, which is an order of magnitude lower than our first estimates, we conclude that it is not necessary to experimentally impose an x-y temperature variation at an axial level in the XR2 tests. This added experimental complication would not be justified by the small calculated planar temperature differences.

As shown in Table 4.1 and Figure 4.6, the predicted coreplate and nosepiece temperatures are significantly lower than the first core node temperatures. The core is represented by SCDAP components while the coreplate and nosepiece are RELAP5 heat structures. In reality, there would be radiant and conductive heat transfer from the core to these structures; but within the SCDAP/RELAP5 framework, these energy transfer mechanisms are not modeled. (RELAP5 heat structures are heated or cooled only by convection with the fluid.) Thus, these predicted temperatures are the minimum expected for these coreplate and nosepiece structures. During the heatup phase for the XR2 tests, these structures will realistically attain higher temperatures due to the radiant and conductive heat transfer with the core nodes.

4.3 BOUNDARY CONDITIONS

SCDAP/RELAP5 control functions were developed to account for the remaining intact control blade/canister structures in the top 3.35 m (11 feet) of the core (these control functions were also scaled to the cross-sections of the XR2 tests with 72 fuel rods as shown in Figure 2.5). Figure 4.11 illustrates the structural volume decrease for the control blade and channel box after 125.2 min. Figure 4.12 gives the relocated cladding mass into the lower 0.46 m of the core.

Given Figures 4.11 and 4.12 and some simplifying linearizations of these curves, the best estimate melt flow rates into the experimental XR2 test section are given in Table 4.3. Table 4.3 separates the metallic "pours" into stainless steel/B₄C and Zircaloy with further division of the Zircaloy into channel box and cladding flows.

As shown in Figures 4.11 and 4.12, melt relocation into the lower core (0.46 m) is essentially completed by 170 min.

**Table 4.1. Lower core structure temperatures at 125.2 min
(see Figure 4.5 for component guide)**

Elevation of Center of Node Above Vessel 0						
(in.)	206.4	211.9	219.3	225.3	231.3	237.3
Elevation of Center of Node Above BAF						
(in.)	-9.90	-4.40	3.00	9.00	15.00	21.00
(cm)	-25.1	-11.2	7.6	22.9	38.1	53.3
Temperatures (K)						
Core Plate	413.9					
Nose Piece		438.3				
Blade Sheath			822.4	1141.6	1368.3	1479.8
Seg. 1 Box			861.5	1168.4	1395.4	1505.7
Seg. 2 Box			869.5	1179.4	1414.3	1525.8
Seg. 1 Rods			895.7	1199.2	1417.5	1524.9
Seg. 2 Rods			897.4	1201.9	1423.2	1531.2
Hot Rods			905.5	1209.1	1425.7	1532.0

Table 4.2. Fuel Assembly Structural Temperature *Differences* Just Before Relocations into Lower Core

Node	Midpoint Elevation (in. above BAF)	Hot Rod Temperature (K)	ΔT_{max} (hot rod-wall rods) (K)	$\Delta T_{canister}$ (seg 2-seg 1) (K)
4	21.0	1523.0	7.1	20.1
3	15.0	1425.7	8.2	18.9
2	9.0	1209.1	9.9	11.0
1	3.0	905.5	9.8	8.0

**Table 4.3. Best estimate melt flow rates into the XR2 test section
(where time = 0, when melt is first introduced into the test section)**

Stainless Steel/B₄C:

Time Frame (s)	Flow Rate (g/s)
0-590	17.3
590-980	6.8
980-2600	1.7
>2600	0

**Zircaloy:
Channel Box**

Time Frame (s)	Flow Rate (g/s)
0-907	0
907-2410	17.2
>2410	0

Cladding

Time Frame (s)	Flow Rate (g/s)
0-1037	0
1037-2600	23.4
>2600	0

Total Stainless Steel/B₄C: ~15.6 Kg
 Total Zircaloy : ~62.4 Kg

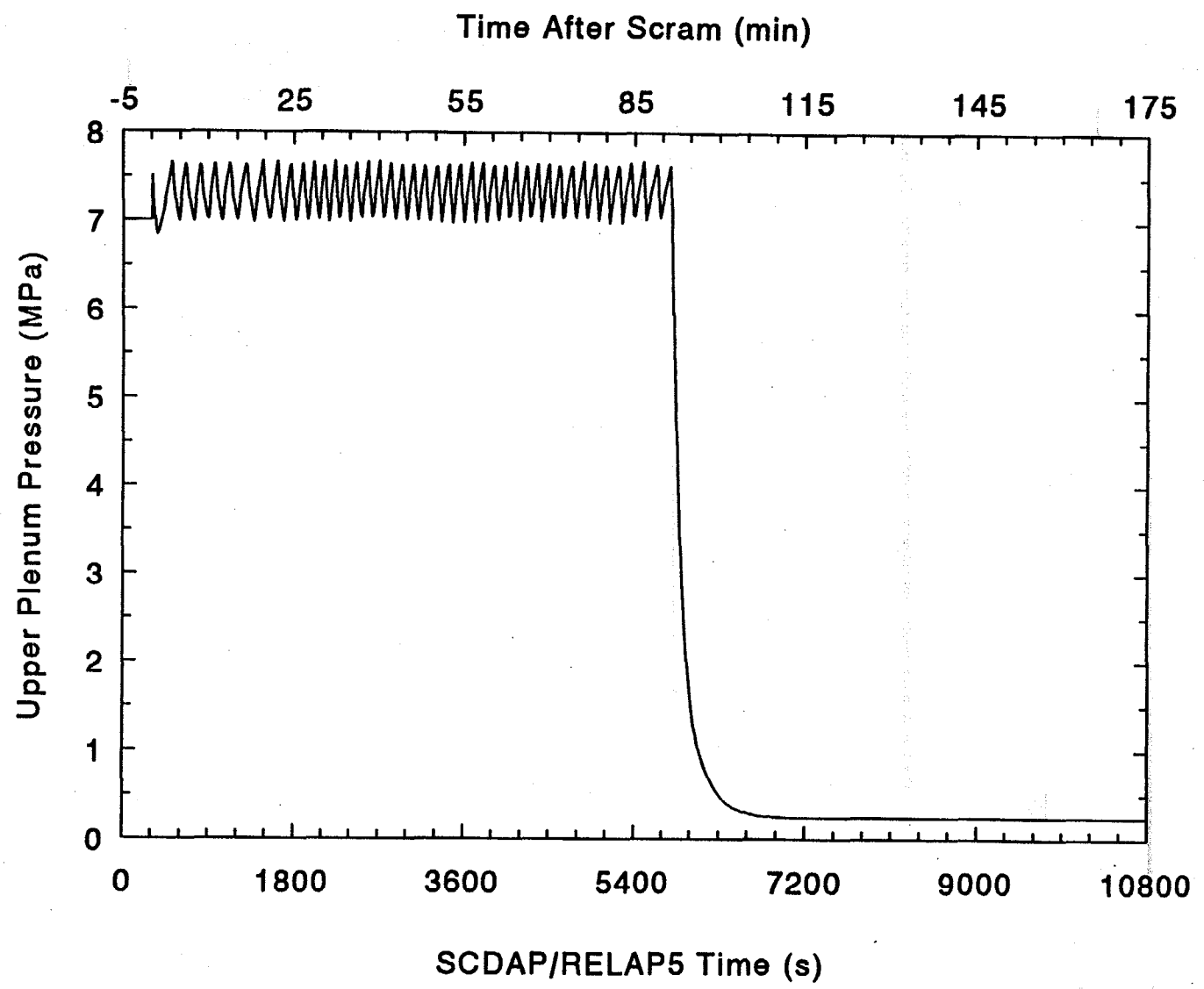


Figure 4.1. Predicted vessel pressure for Browns Ferry STSB.

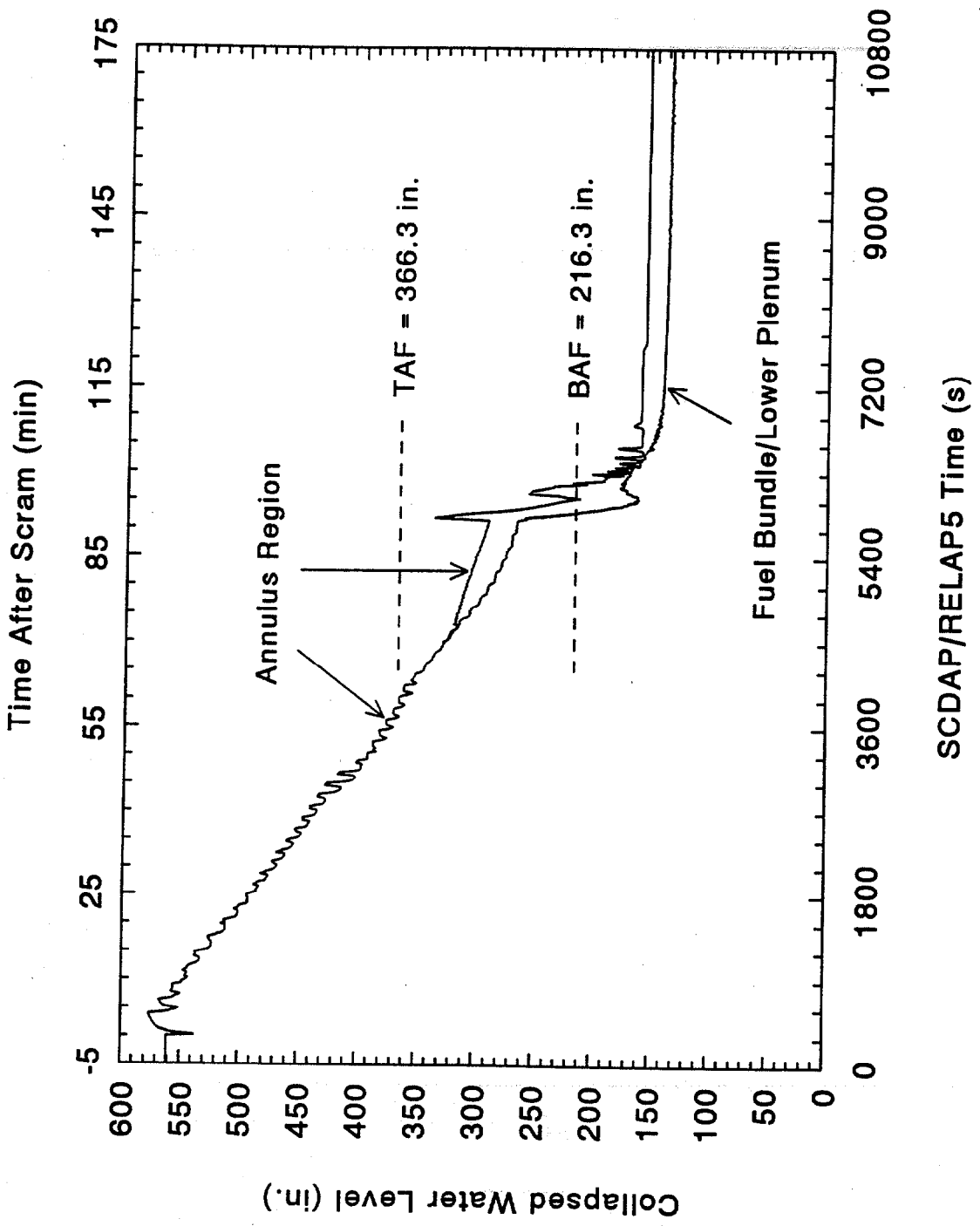


Figure 4.2. Predicted vessel water levels for Browns Ferry STSB.

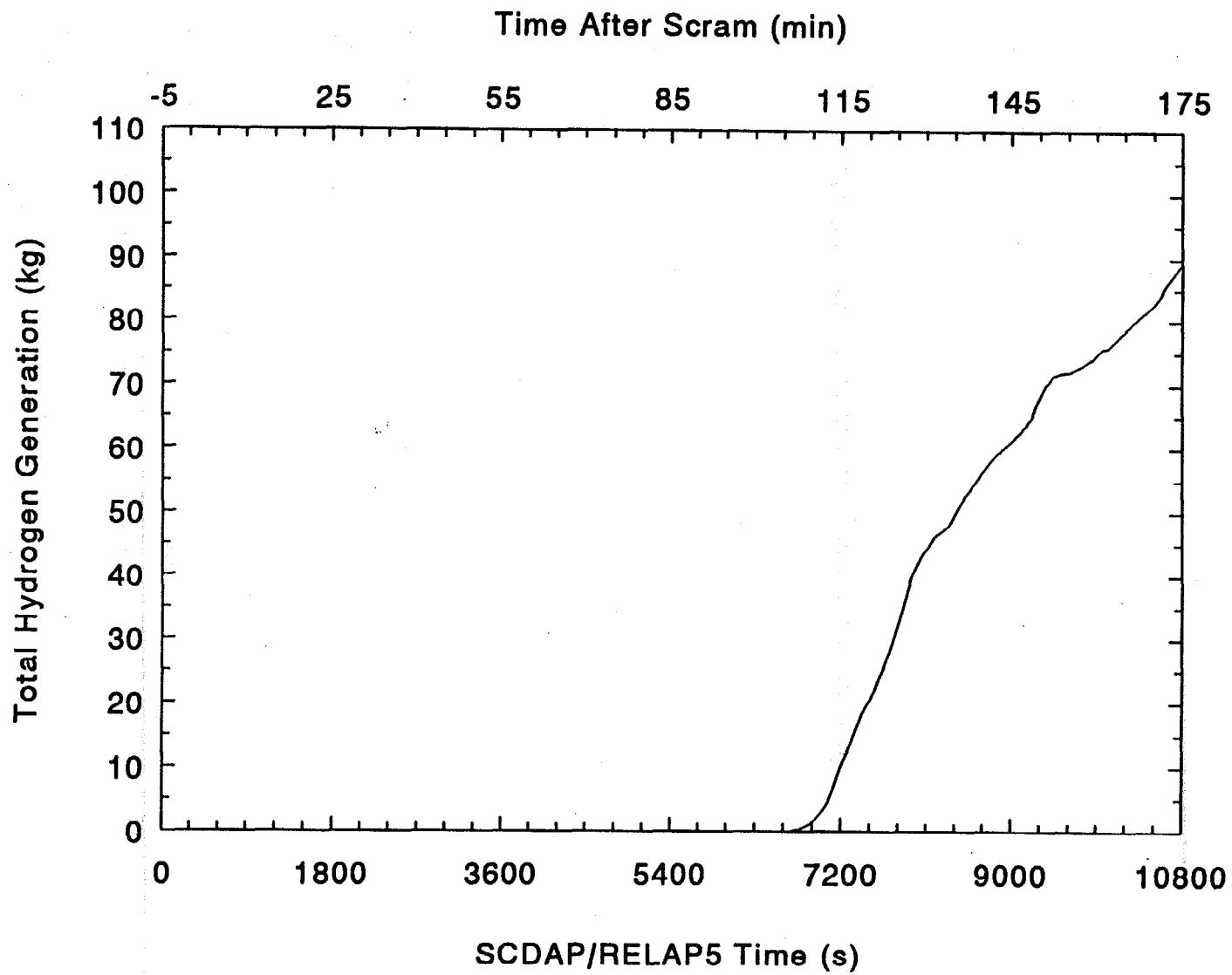


Figure 4.3. Predicted hydrogen generation for Browns Ferry STSB.

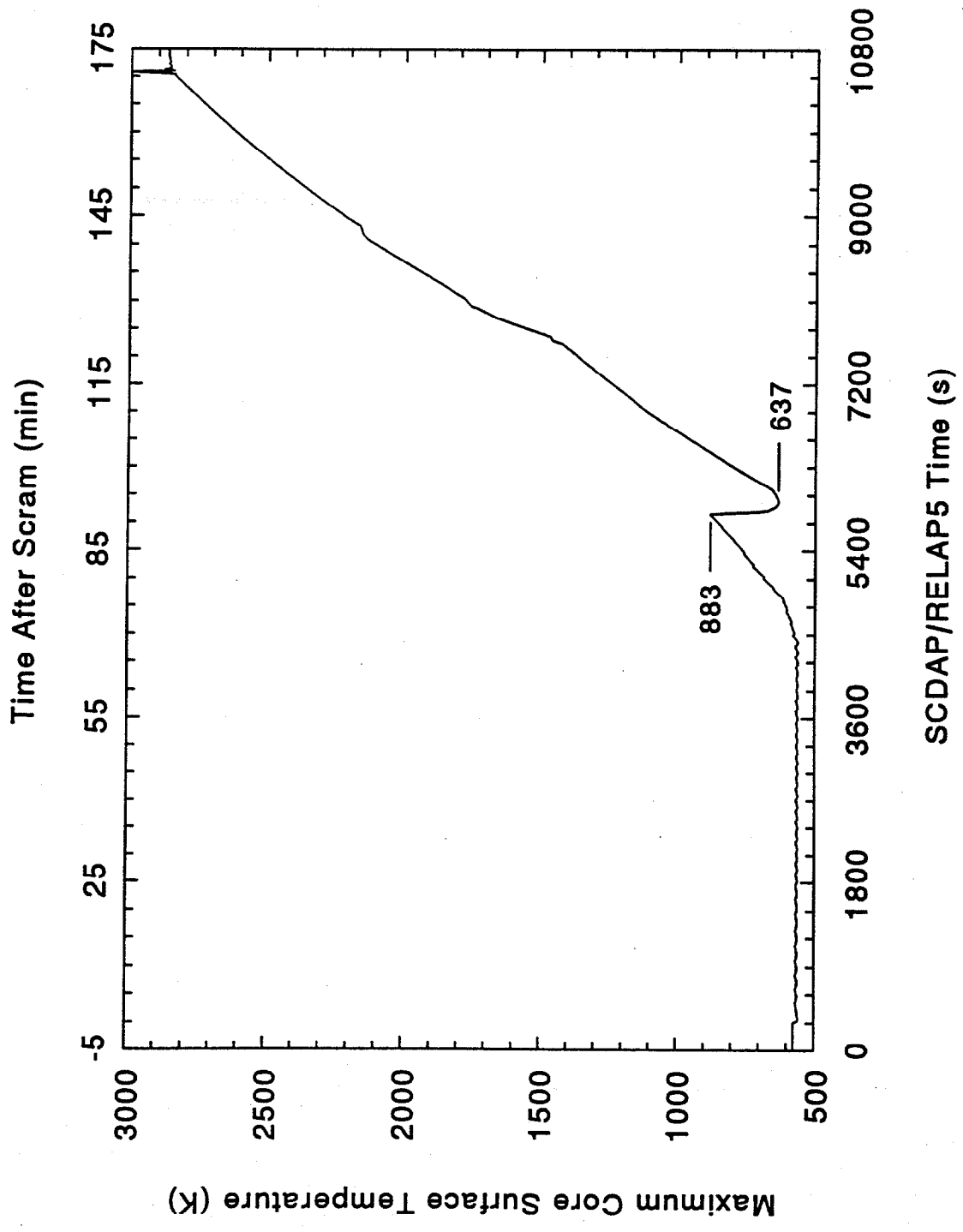


Figure 4.4. Predicted maximum core temperature for Browns Ferry STSB.

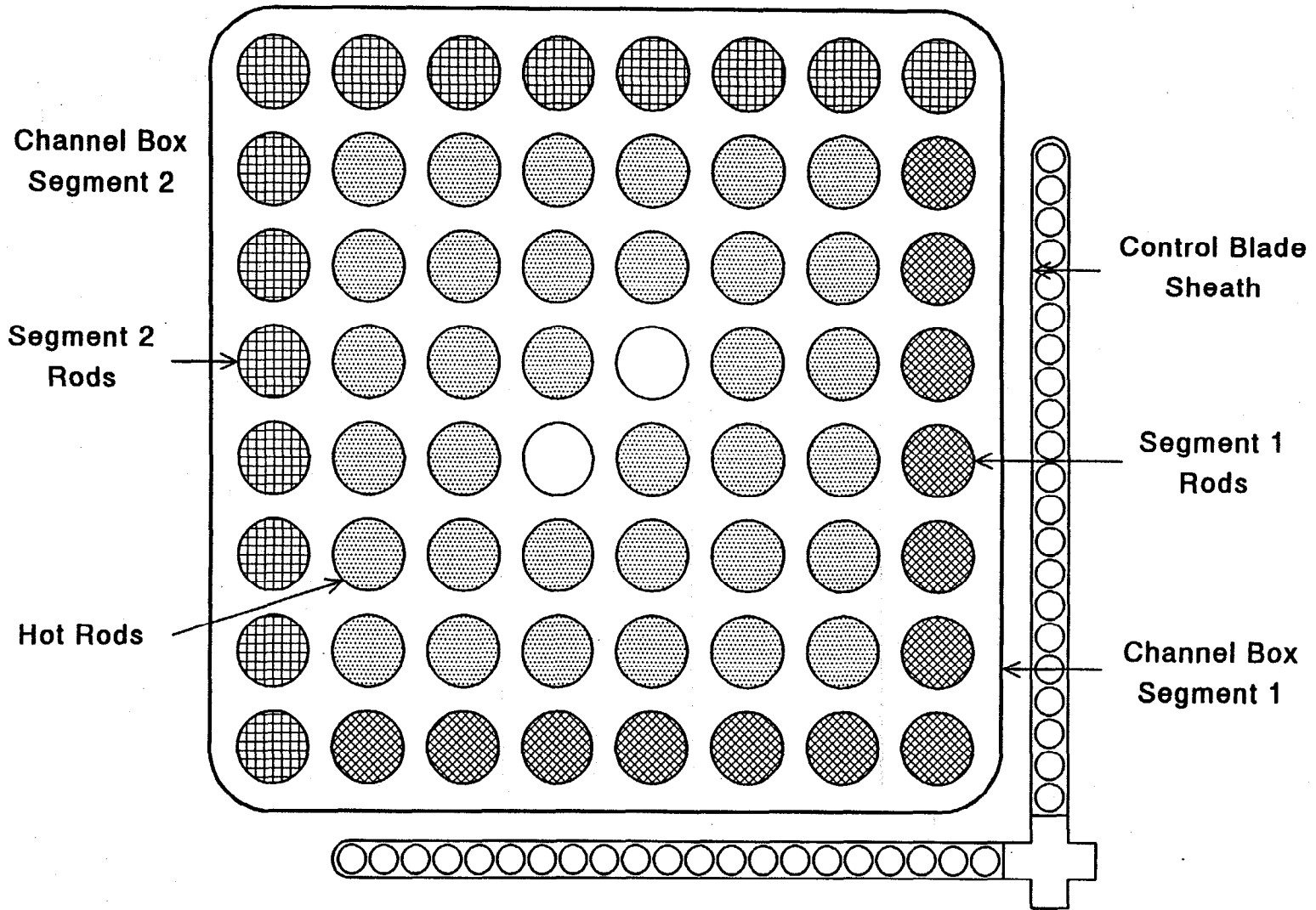


Figure 4.5. Component guide for detailed Browns Ferry SCDAP model.

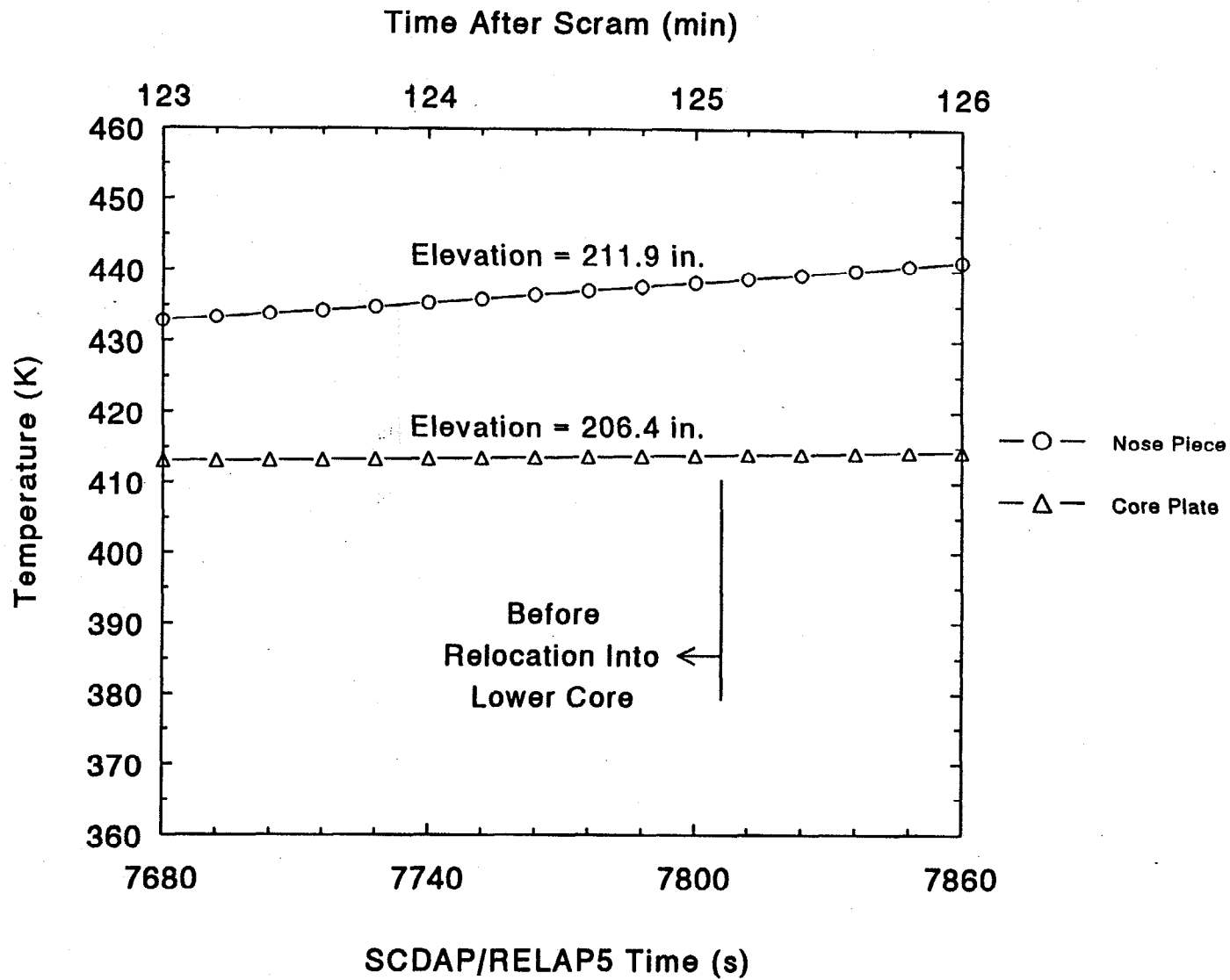


Figure 4.6. Predicted nose piece and core plate temperatures (123-126 min).

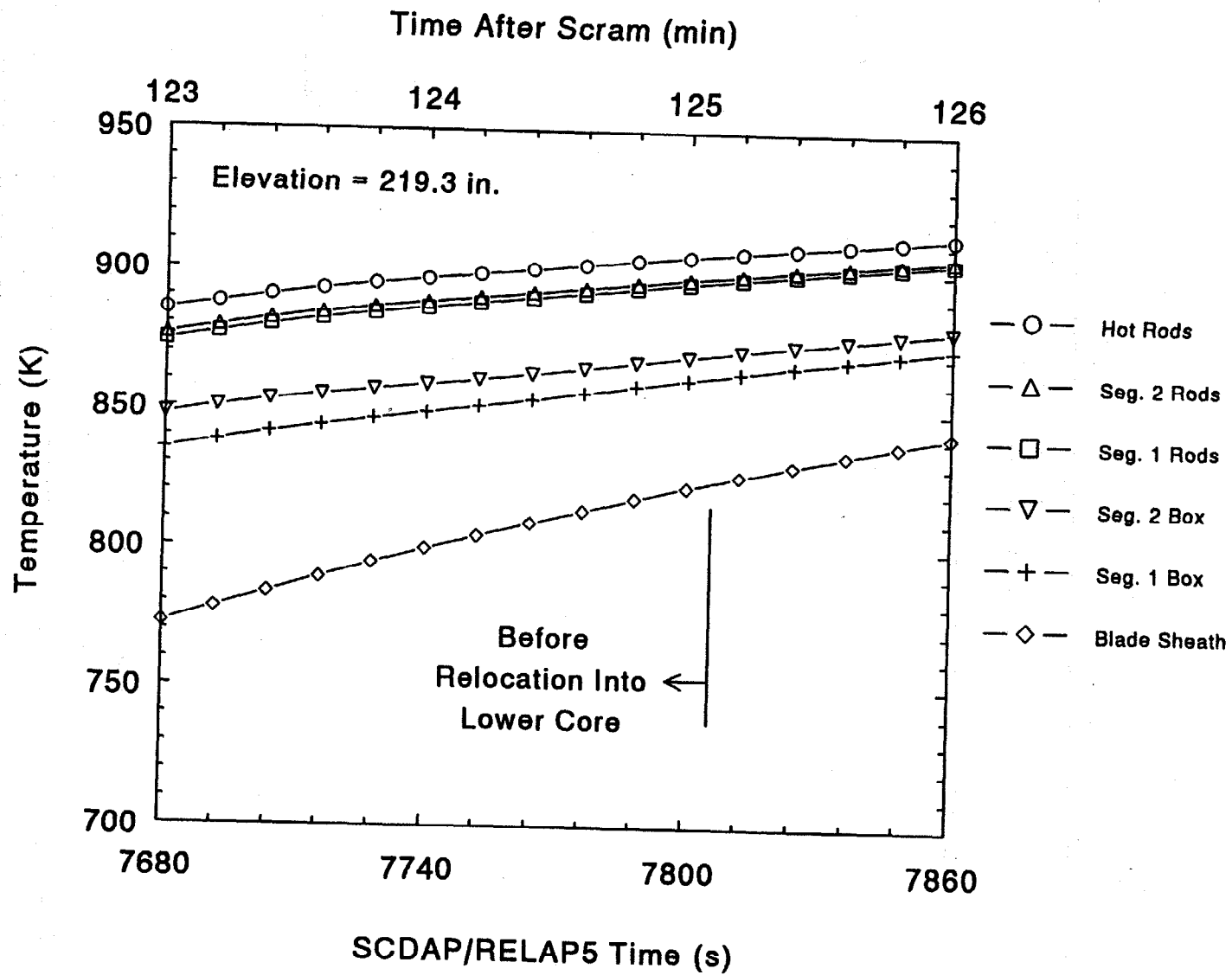


Figure 4.7. Predicted core axial node 1 temperatures (123-126 min).

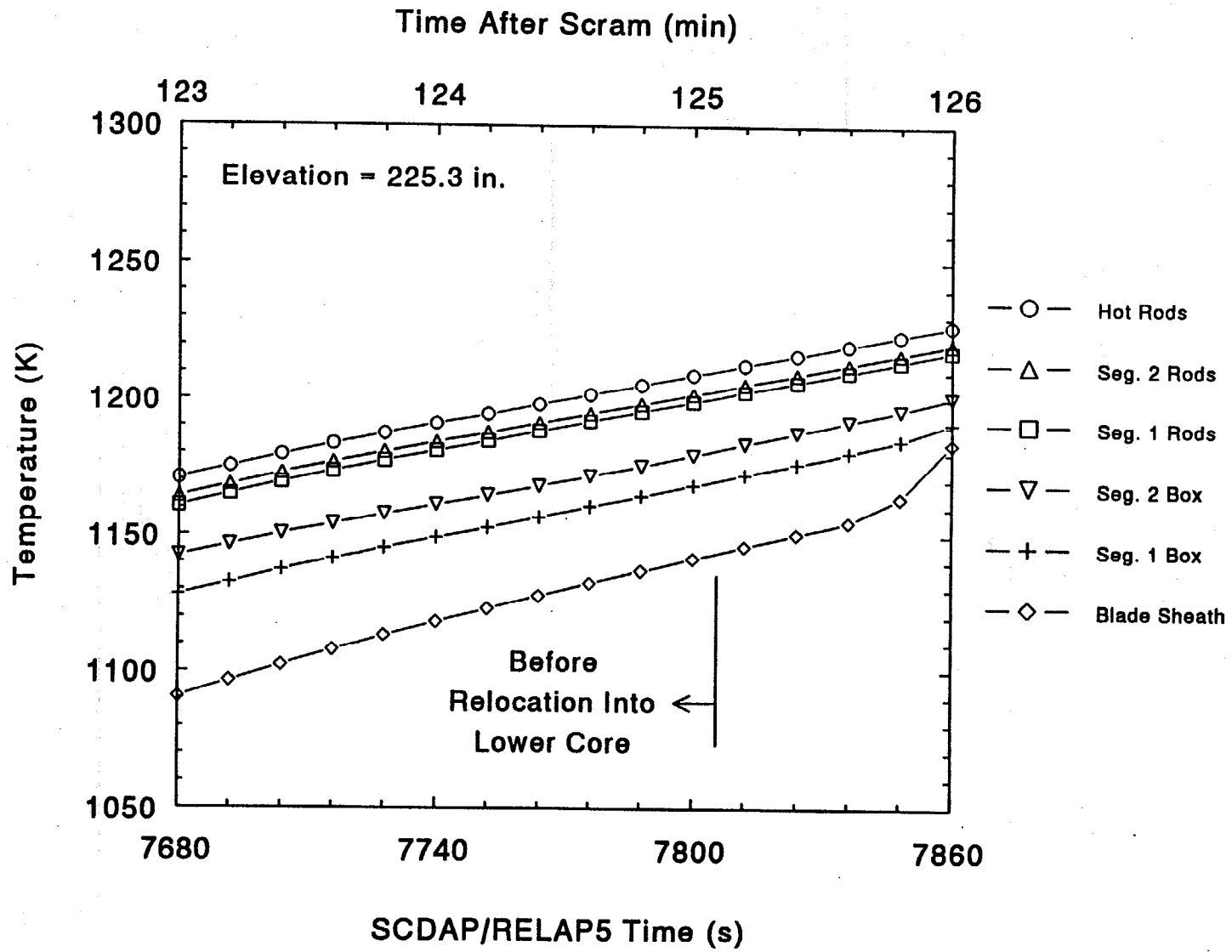


Figure 4.8. Predicted core axial node 2 temperatures (123-126 min).

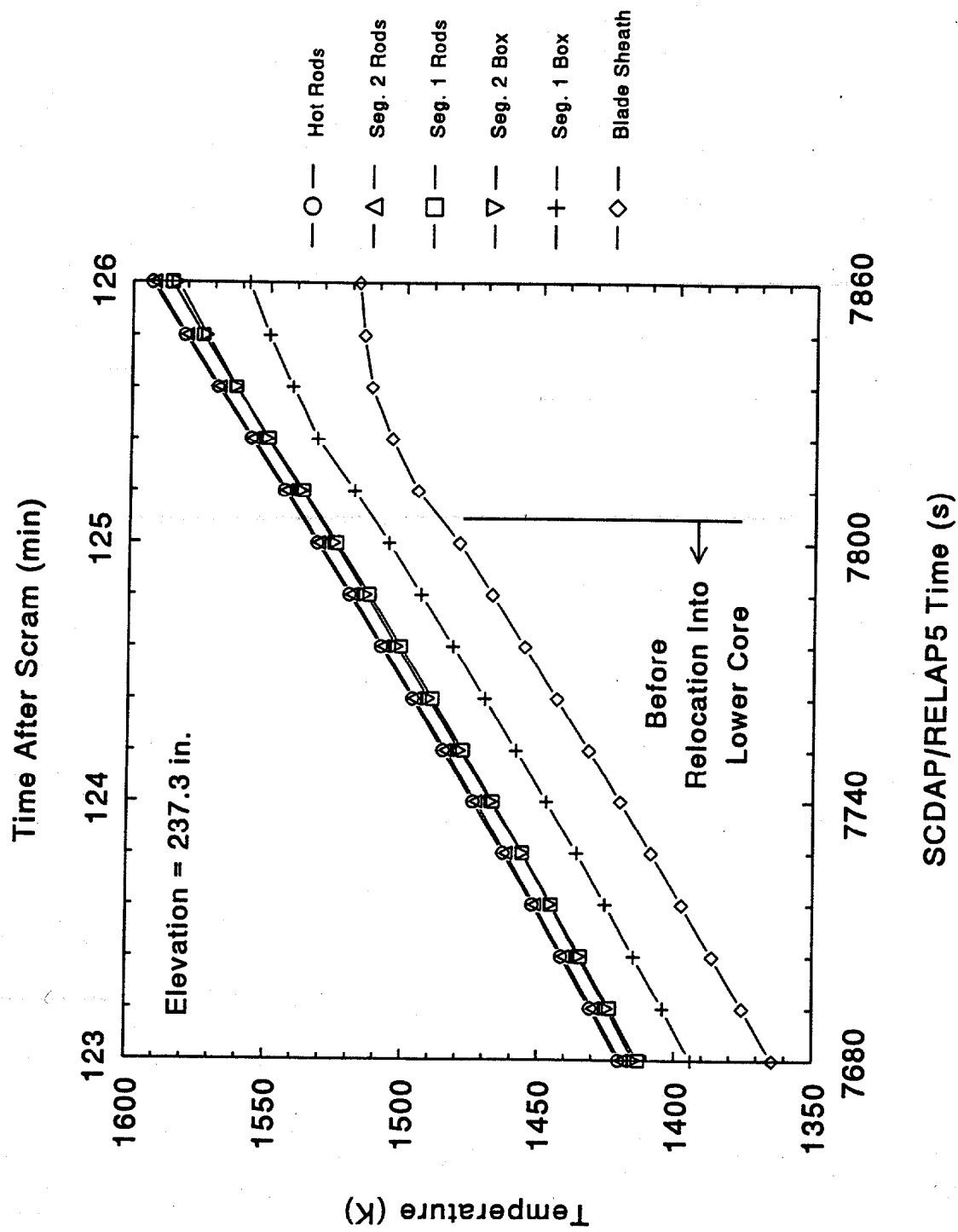


Figure 4.10. Predicted core axial node 4 temperatures (123-126 min).

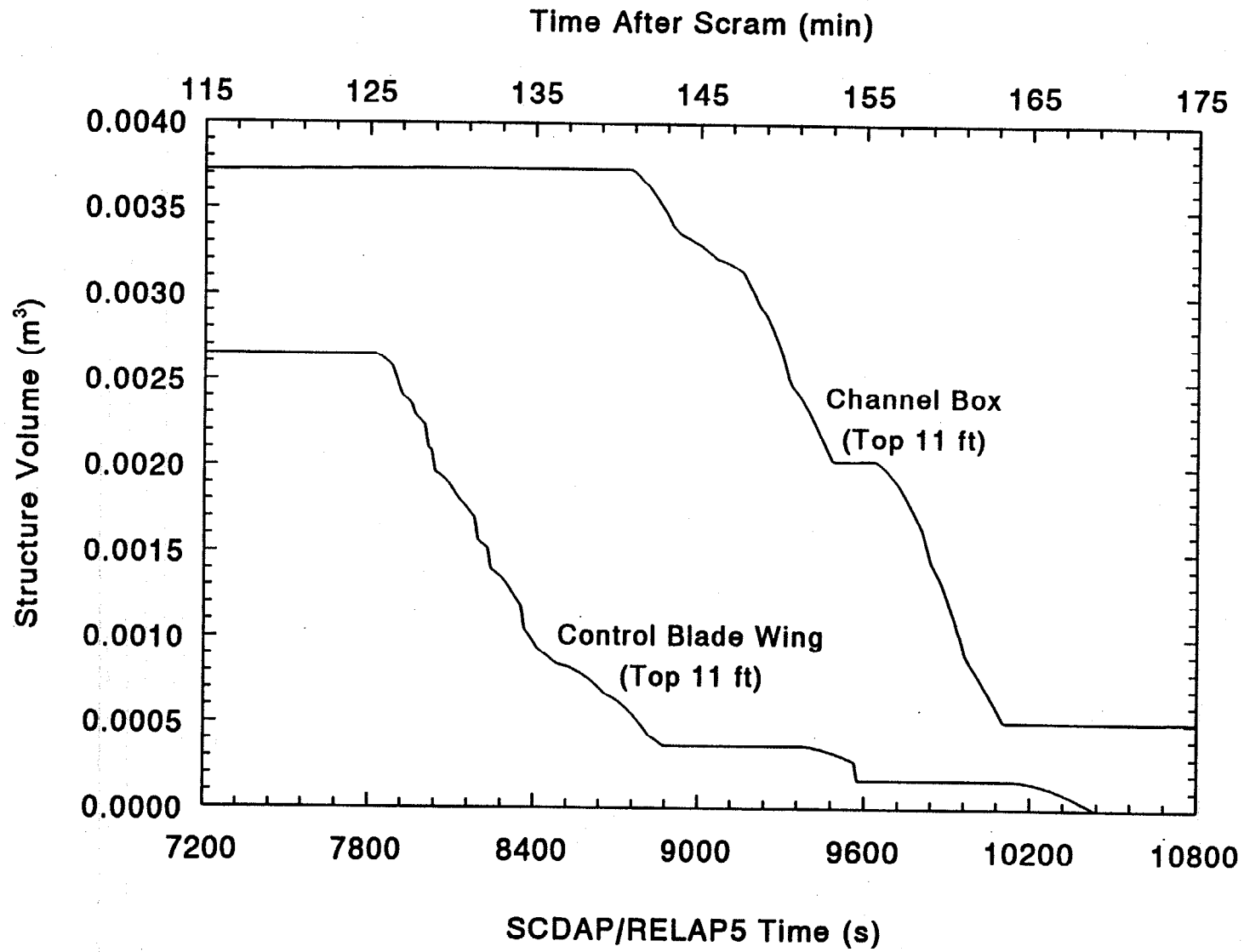


Figure 4.11. Structural volume remaining in the top 11 ft (3.35 m) of the core.

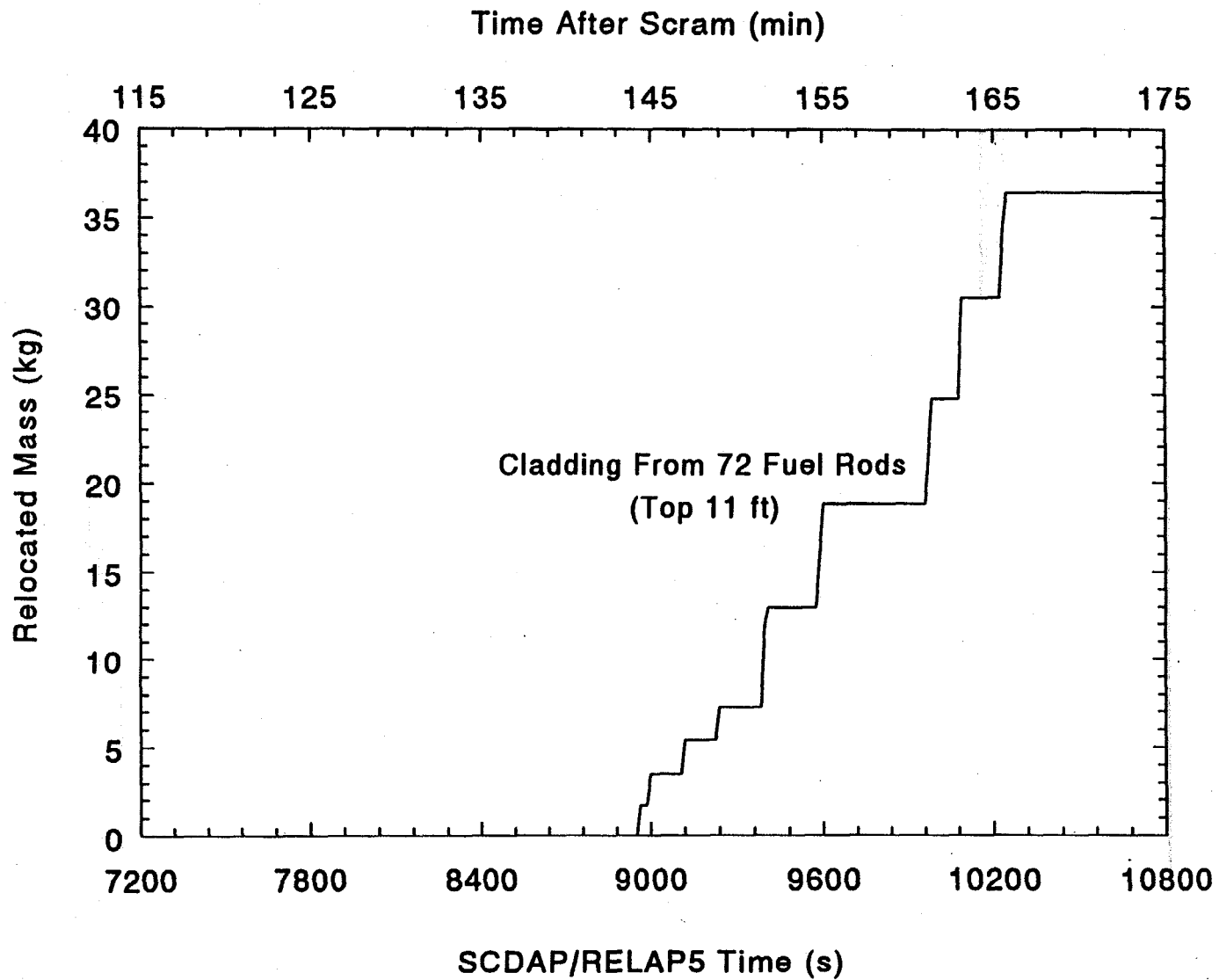


Figure 4.12. Cladding mass relocated into the bottom 1.5 ft (0.46 m) of the core.

5. SUMMARY

The ex-reactor (XR) experiments at SNL are designed to resolve phenomenological uncertainties concerning the behavior of relocating metallic melts draining into the lower regions of a dry BWR core as a result of a core-melt accident. The experiments are intended to determine under what conditions the metallic melts would form in-core blockages and under what conditions draining into the lower plenum would occur. The experiments specifically address the dry core accident associated with depressurized BWR core melt accidents where rapid vessel blowdown has lowered the water level below the core plate.

Two preliminary tests (with simplified geometries) in the ex-reactor program were completed in 1993. In January of 1994, the NRC convened an expert peer review committee to assess the completed XR1 tests and the proposed complicated and expensive XR2 experiments. The committee unanimously endorsed proceeding with the XR2 tests, but recommended that augmented XR2 planning include a firm, documented, analytical basis for the initial and boundary conditions.

In response to the expert peer review comments, a best estimate SCDAP/RELAP5 simulation of a BWR "dry core" accident scenario (the STSB sequence for Browns Ferry) was performed by the ORNL BEAMD program (JCN W6202). This simulation provides the best estimate initial and boundary conditions for the XR2 experiments. The initial test section thermal conditions are given in Section 4.2 and the metallic melt relocation rates (boundary conditions) are presented in Section 4.3.

The ORNL "detailed" SCDAP/RELAP5 model of the BWR fuel assembly allowed the determination of the transient structural temperature differences at an axial plane within the fuel assembly. The maximum predicted temperature difference across the fuel assembly at incipient control blade liquefaction was 20 K. It is concluded that it is not necessary to impose experimentally an x-y temperature variation at an axial level during the initial heatup of the XR2 test section.

Liasion with the SNL staff for the XR2 experiment confirms that the information developed by this program and described in this report meets all requirements for planning of the experimental procedure.

6. REFERENCES

1. S. A. Hodge and L. J. Ott, *Boiling Water Reactor Severe Accident Response (BWRSAR) Code Description and Assessment*, Letter Report to Dr. Thomas J. Walker, Division of Systems Research, RES, USNRC, February 1, 1989.
2. R. O. Gauntt, R. D. Gasser, and L. J. Ott, *The DF-4 BWR Control Blade/Channel Box Fuel Damage Experiment*, NUREG/CR-4671, SAND86-1443, November 1989.
3. L. J. Ott, *Post-Test Analysis of the DF-4 BWR Experiment Using the BWRSAR/DF-4 code*, Letter Report to Dr. T. J. Walker, Division of Systems Research, RES, USNRC, August 10, 1989.
4. L. J. Ott, *Post-Test Analysis of the CORA-16 and CORA-17 BWR Experiments*, Letter Report (ORNL/NRC/LTR-92/17) to Dr. A. Behbahani, Accident Evaluation Branch, Division of Systems Research, RES, USNRC, July 10, 1992.
5. L. J. Ott, *Post-Test Analysis of the CORA-31 Slow Heatup BWR Experiment*, Letter Report (ORNL/NRC/LTR-92/29) to Dr. A. Behbahani, Accident Evaluation Branch, Division of Systems Research, RES, USNRC, December 31, 1992.
6. L. J. Ott, *Post-Test Analysis of the CORA-33 Dry Core BWR Experiment*, Letter Report (ORNL/NRC/LTR-93/21) to Dr. A. Behbahani, Accident Evaluation Branch, Division of Systems Research, RES, USNRC, August 31, 1993.
7. L. J. Ott, *Post-Test Analysis of the CORA-28 Preoxidized BWR Experiment*, Letter Report (ORNL/NRC/LTR-93/26) to Dr. A. Behbahani, Accident Evaluation Branch, Division of Systems Research, RES, USNRC, September 30, 1993.
8. R. M. Summers and R. K. Cole, *MELCOR 1.8.3: A Computer Code Manual, Vol. 1, Primer and User's Guide*, May, 1994.
9. K. L. Davis, editor, *SCDAP/RELAP5/MOD3.1 Code Manual - Volume II: Damage Progression Model Theory*, NUREG/CR-6150, EGG-2720, October 1993.
10. F. P. Griffin and K. A. Smith, *BWR Control Blade/Channel Box Interaction and Melt Relocation Models for SCDAP*, Letter Report (ORNL/NRC/LTR-92/12/R1) to Dr. Yi-Shung Chen, Accident Evaluation Branch, Division of Systems Research, RES, USNRC, December 31, 1992.
11. F. P. Griffin, *BWR Control Blade/Channel Box Interaction and Melt Relocation Models for SCDAP*, Letter Report (ORNL/NRC/LTR-92/12/R2) to Dr. Yi-Shung Chen, Accident Evaluation Branch, Division of Systems Research, RES, USNRC, December 30, 1993.
12. S. A. Hodge, et al., *Identification and Assessment of BWR In-Vessel Severe Accident Mitigation Strategies*, USNRC Report, NUREG/CR-5869 (ORNL/TM-12080), October 1992.
13. R. O. Gauntt, et al., *A Program Plan for the Ex-Reactor Metallic Melt Relocation Experiment*, Letter Report to NRC Technical Monitor (Dr. R. W. Wright), June 22, 1990.
14. K. O. Reil, "Ex-Reactor Melt Progression Experiments," *1993 Cooperative Severe Accident Research Program Review Meeting*, Bethesda, Maryland, May 3-7, 1993.
15. R. O. Gauntt, "First Results from the Ex-Reactor Metallic Melt Relocation and Blockage Experiments," *1993 International CORA Workshop*, KfK, Karlsruhe, Germany, September 27-29, 1993.

16. R. O. Gauntt, *Quick Look Report on the XR1-1 Test Examining Metallic Core-Melt Relocation in Boiling Water Reactor Geometry*, Sandia National Laboratories' Letter Report to Dr. R. W. Wright (NRC Technical Monitor), August 24, 1993.
17. R. O. Gauntt, *Quick Look Report on the XR1-2 Test Examining Metallic Core-Melt Relocation in Boiling Water Reactor Geometry*, Sandia National Laboratories' Letter Report to Dr. R. W. Wright (NRC Technical Monitor), December 3, 1993.
18. S. S. Dosanjh, *Melt Propagation in Dry Core Debris Beds*, Nuclear Technology, Vol.88 No.1 (1989).
19. R. C. Schmidt, *Porous Media Type Modeling of Late Phase Melt Progression*, Cooperative Severe Accident Research Program Review Meeting, Bethesda, Maryland, May 6-10, 1991.
20. R. M. Ostmeyer, *An Approach to Treating Radionuclide Decay Heating for Use in the MELCOR Code System*, USNRC Report, NUREG/CR-4169 (SAND84-1404), May 1985.
21. J. K. Lovin, et al., *User's Manual for RAVFAC, a Radiation View Factor Digital Computer Program*, Lockheed Missiles and Space Co., Inc., Huntsville Research and Engineering Center, LMSC/HREC D 148620-A, August 1973.
22. E. F. Puccinelli, *View Factor Computer Program (Program View) User's Manual*, Goddard Space Flight Center, X-324-73-272, July 1973.
23. R. M. Harrington and L. C. Fuller, *BWR-LTAS: A Boiling Water Reactor Long-Term Accident Simulation Code*, USNRC Report, NUREG/CR-3764 (ORNL/TM-9163), February 1985.